Design, Synthesis, and In Vitro Activity of Peptidomimetic Inhibitors of Myeloid Differentiation Factor 88

Nicola Fantò,*[,†] Grazia Gallo,[†] Andrea Ciacci,[†] Mauro Semproni,[†] Davide Vignola,[†] Marco Quaglia,[†] Valentina Bombardi,[‡] Domenico Mastroianni,[‡] M. Pia Zibella,[‡] Giancarlo Basile,[‡] Marica Sassano,[‡] Vito Ruggiero,[†] Rita De Santis,[†] and Paolo Carminati[†]

Research and Development, Sigma-Tau Industrie Farmaceutiche Riunite S.p.A., Pomezia (RM), Italy, and Tecnogen S.p.A., 81015 Piana di Monte Verna (CE), Italy

Received June 21, 2007

We describe the design and synthesis of a peptidomimetic library derived from the heptapeptide Ac-RDVLPGT-NH_2, belonging to the Toll/IL-1 receptor (TIR) domain of the adaptor protein MyD88 and effective in inhibiting its homodimerization. The ability of the peptidomimetics to inhibit protein–protein interaction was assessed by yeast 2-hybrid assay and further validated in a mammalian cell system by evaluating the inhibition of NF-κB activation, a transcription factor downstream of MyD88 signaling pathway that allows production of essential effector molecules for immune and inflammatory responses.

Introduction

Among the transcription factors, nuclear factor-κB (NF-κB[a]) is one of the most intensively investigated owing to its involvement in inflammation, immunity, cell proliferation, and apoptosis. NF-κB recognizes consensus sequences for the enhancers of various genes coding for proinflammatory cytokines (TNF, IL-1, IL-2, IL-6, IL-11, IL-17, GM-CSF), chemokines (IL-8, RANTES, MIP-1α, MCP-2), adhesive molecules (ICAM-1, VCAM-1, E-selectin), and enzymes producing inflammatory mediators (iNOS and COX2).[1]

In response to various damaging stimuli, NF-κB activation is observed in almost all cells involved in the immune response: neutrophils, macrophages, lymphocytes, and endothelial, epithelial, and mesenchymal cells. Therefore, the immediate, transitory activation of NF-κB constitutes a characteristic of primary importance in the functioning of the normal physiological response to pathogenic damage. Nevertheless, dysregulation of this finely tuned mechanism, occurring as an excessive, persistent activation, is closely associated with chronic inflammatory diseases.[2]

Recent research lends support to the hypothesis concerning the existence of a common transduction mechanism in the IL-1R/TLR superfamily[3] context. In particular, the adaptor protein, MyD88, seems to play a crucial role in the transduction events triggered by all TLR receptors, (except TLR3) as well as IL-1 and IL-18 receptors.

Therefore, the inhibition of an adaptor protein, such as MyD88, involved in the activation of NF-κB, triggered by signals from receptors that recognize distinct ligands but share the same transduction pathway, is expected to be more effective, in principle, than inhibition of individual ligand activities. On alignment of the primary sequences of the TIR domains of the IL-1R/TLR and MyD88 receptors, one of the conserved zones consists of a loop between the second β-strand and the second α-helix (BB loop) whose consensus sequence is RDXΦ1Φ2GX, where X is any amino acid and Φ1Φ2 are two hydrophobic ones. We were the first to demonstrate that the heptapeptide, Ac-RDVLPGT-NH_2, derived from the TIR domain of MyD88, was effective in inhibiting its homodimerization.[4] Subsequent studies carried out by different groups corroborated our initial results in additional experimental settings.[5,6]

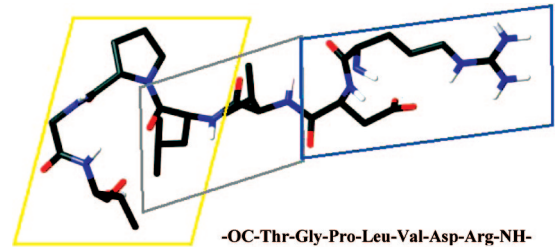

Figure 1. Schematic representation of the three different portions that characterize the consensus peptide (yellow = β-turn; grey = hydrophobic spacer; blue = charged portion).

Protein–protein interaction as target of small molecule inhibitors still represents a challenging task.[7] The recent identification of a crucial subregion of MyD88 TIR domain[4] provides a good starting point to mimic, though it must be emphasized that the intracellular location of the target hinders the use of peptides and represents an additional barrier to the druggability of candidate structures.

The present study aimed at identifying mimetics of this particular portion of MyD88, which might interfere with its homodimerization. This would make it possible to prevent recruitment of MyD88 to each of the IL-1R/TLR receptors, thus interfering with their signaling and proving the effectiveness of this approach.

Results and Discussion

Library Enumeration. Figure 1 illustrates the strategy for constructing mimetics of the consensus peptide of MyD88 TIR domain; the structure of the consensus peptide is subdivided into three distinct portions: (a) a charged portion consisting of the Arg-Asp amino acids, (b) a hydrophobic portion consisting

* To whom correspondence should be addressed. Phone: 39-6-9139-3445. Fax: 39-6-9139-3638. E-mail: nicola.fanto@sigma-tau.it.
† Sigma-Tau Industrie Farmaceutiche Riunite S.p.A.
‡ Tecnogen S.p.A.

[a] Abbreviations: TIR, Toll/IL-1 receptor; MyD88, myeloid differentiation factor 88; NF-κB, nuclear factor-κB; IL, interleukin; IL-1R, interleukin-1 receptor; TLR, toll-like receptor; 2HyS, 2-hybrid system; AD, activation domain; BD, binding domain; UAS, upstream activation sequence; COSY, correlation spectroscopy; HSQC, heteronuclear single-quantum correlation; HMBC, heteronuclear multiple-bond coherence.

10.1021/jm070723u CCC: $40.75
Published on Web 02/15/2008

Table 1. Selection of 18 Commercially Available Arginine Mimetic Groups

Name	MW	Structure	Name	MW	Structure
AM1	179.2	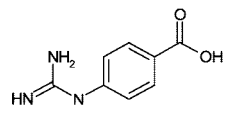	PAM3	186.6	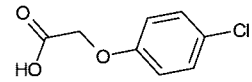
AM2	141.1	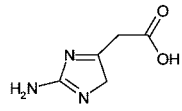	PAM4	221.0	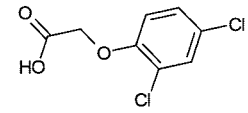
AM3	128.1	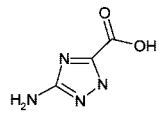	PAM5	218.2	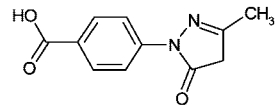
AM4	193.2	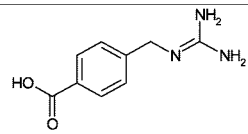	PAM6	138.1	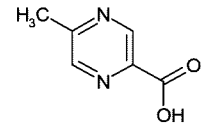
AM5	164.2	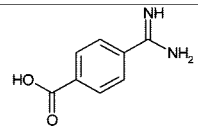	PAM7	142.2	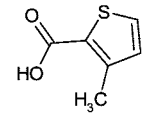
AM6	207.2	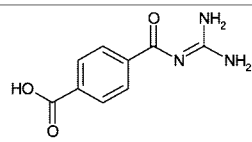	PAM8	186.2	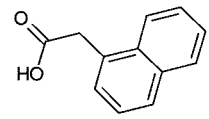
AM7	180.2	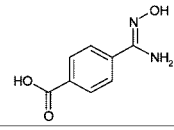	PAM9	123.1	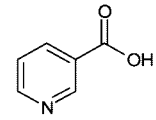
AM8	130.2	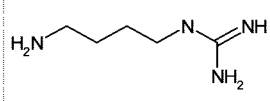	PAM10	124.1	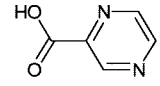
AM9	150.2	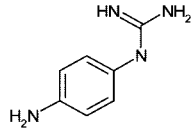	PAM11	173.2	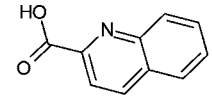

of the Val-Leu amino acids, and (c) a β-turn portion consisting of the Leu-Pro-Gly-Thr amino acids.

For each of these portions, a certain type of mimetic was chosen to be substituted alternatively or simultaneously in the consensus peptide sequence, maintaining the amide bond as the functional link between the three groups.

Table 1 shows the 18 commercially available arginine mimetic groups used, where a hydrophobic structure contains a functional group that modulates basicity from that of arginine to zero. There is a hydrophobic spacer covering the distance between arginine and proline, with a limited number of rotational degrees of freedom and an aromatic linker ring differently substituted and functionalized, where only one carboxylic acid group and one primary amine group is present and engaged in an amide bond. Table 2 shows the 39 commercially available spacers used. Table 3 shows that the central portion of the β-turn (Pro-Gly) is substituted with 10 different β-turn mimetics.[8–11]

When combining all the building blocks, 4368 direct and 234 retroinverse peptidomimetics may be obtained. Therefore, we chose to restrict the number of compounds and synthesize a diverse but representative set. A virtual library was then enumerated, and molecules possessing more than one violation of the "rule of five"[12] were removed. Building blocks showing bad superposition on the 3D structure of the BB-loop, poor reactive groups, and high toxicity groups were also removed.

The final scaffold selection on the remaining 1946 molecules was then realized by an experimental design (Onion/D-optimal design, Figure 2),[13] where the EVA structural descriptors,[14] based on calculated fundamental molecular vibrational frequencies, were used.

Chemistry. A diverse library of 83 molecules was selected (Table I, Supporting Information) and then synthesized by solid-phase synthesis. Chart 1 shows the structures of a

Table 2. Selection of 39 Commercially Available Hydrophobic Spacers

Name	MW	Structure	Name	MW	Structure
SP1	143.2	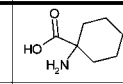	SP21	158.2	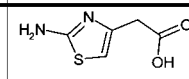
SP2	167.2	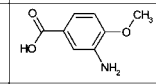	SP22	207.1	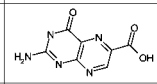
SP3	127.1	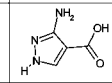	SP23	241.5	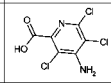
SP4	138.1	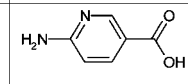	SP24	163.2	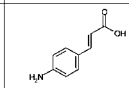
SP5	209.1	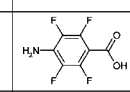	SP25	167.2	
SP6	171.6	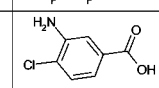	SP26	139.2	
SP7	275.7	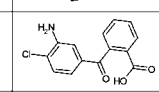	SP27	201.6	
SP8	514.8	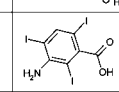	SP28	206.0	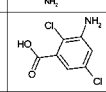
SP9	388.9	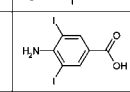	SP29	180.2	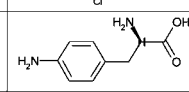
SP10	241.2	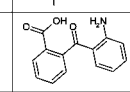	SP30	151.2	
SP11	151.2	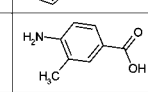	SP31	151.2	
SP12	151.2	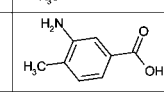	SP32	191.1	
SP13	171.6	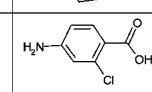	SP33	128.1	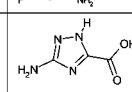
SP14	137.1	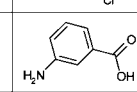	SP34	195.2	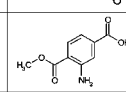
SP15	171.6	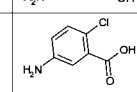	SP35	171.6	
SP16	180.2	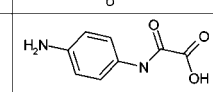	SP36	143.2	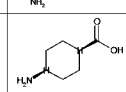
SP17	194.2	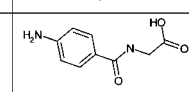	SP37	227.6	
SP18	137.1	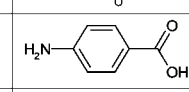	SP38	187.2	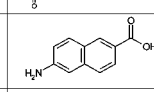
SP19	151.2	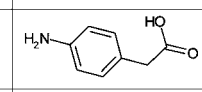	SP39	151.2	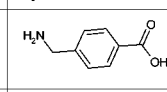
SP20	208.2	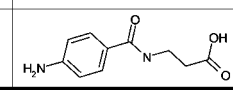			

reference compound **1**[15] and molecules having the best biological results. Schemes 1−3 condense the synthetic strategies to prepare all molecules. Schemes 2 and 3 show synthesis examples of direct **2** and retro **3** peptidomimetics. Each peptidomimetic sequence was synthesized on polymer-supported (aminomethyl)polystyrene (Rink amide) using standard Fmoc protocols.

The building blocks, useful for the synthesis of peptidomimetic compounds containing the β-turn mimetics, were synthesized using methods described in the literature[8−11] and

Table 3. Selection of 10 β-Turn Mimetics

Name	MW	Structure
BETA1	198.2	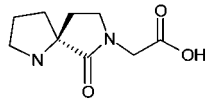
BETA2	198.2	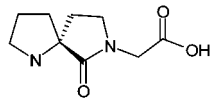
BETA3	212.3	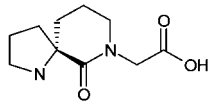
BETA4	242.3	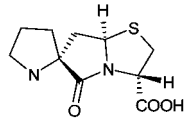
BETA5	274.3	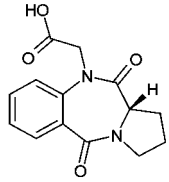
BETA6	290.3	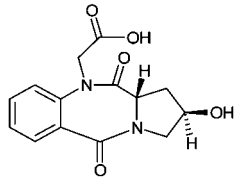
BETA7	310.3	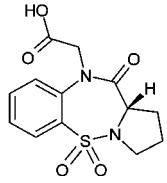
BETA8	256.3	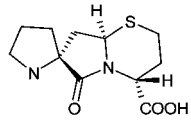
BETA9	256.3	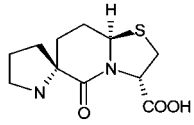
BETA10	186.2	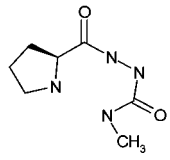

modified using the methods described below, as shown in Schemes 4−6.

Biological Results. The primary screening was first performed by using a 2-hybrid system (2HyS) in yeast *Saccharomyces cerevisiae* to evaluate the inhibition of MyD88 homodimerization and then, by means of a secondary functional test, to evaluate the inhibition of NF-κB in HeLa cells.

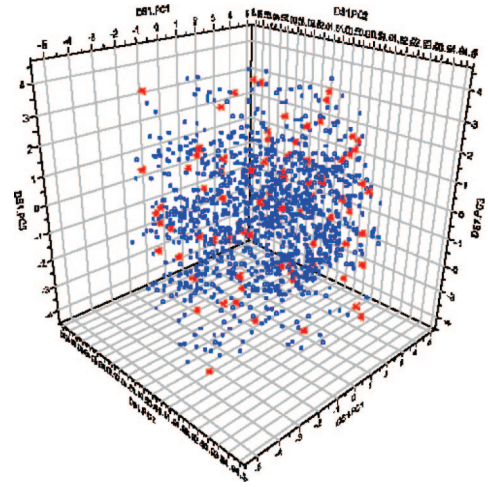

Figure 2. Selection of 83 compounds (red points) by an onion/D-optimal design. A total of 3 of 20 principal components are represented for clarity.

The 2HyS is based on an ability to reconstitute the GAL4 transcription factor, in vitro, which can be divided into two functional domains: the activation domain (AD) and the binding domain (BD).[16] When these two domains are fused with two proteins capable of interacting, the result is a functional reconstitution of GAL4 which, in turn, activates transcription of a number of reporter genes under the control of its own upstream activation sequence (UAS). Transcription of the reporter genes under control of the UAS of GAL4 permits the synthesis of enzymes important for growth in selective medium. The assay is carried out by using 384-well plates, where the wells are coated with a silicone matrix incorporating a fluorescent substance, the emission of which is sensitive to oxygen levels.[17] When an interaction occurs between the two proteins fused with the GAL4 BD and AD domains, respectively, yeast is able to grow in the selective medium, consuming oxygen. Hence, the emitted fluorescence, which increases proportionately over time, can be detected by using a suitable fluorescence reader. If the yeast grows in the presence of molecules capable of inhibiting this interaction, transcription of the reporter genes abates, slowing down the ability to grow in minimal medium with consequent reduction of the fluorescence signal. The fluorescence growth curves generated by the 2HyS were analyzed by means of a system specifically elaborated for this type of investigation (Chrysallis s.a.s.). The software provides quantitative parameters capable of describing the characteristics of the individual curves. In particular, seven different descriptors were used: plateau slope and height, plateau range, growth time, time to grow to 50% of plateau height, "hump" factor, and sigmoidal τ. Through these quantitative parameters, it is possible to obtain a multidimensional representation of the set of experimental curves, and after using extraction techniques by principal component analysis, a two-dimensional representation of the data is constructed to highlight, as clearly as possible, the differences between the curves. This type of representation allows identification of clusters of curves with similar behavior and a clear indication of which curves are generated by compounds influencing oxygen consumption and, thus, yeast growth.

Activation of NF-κB is an event that takes place downstream of MyD88 homodimerization and recruitment, through its TIR domain, to activated receptor complexes. The ability of compounds that inhibited activation of NF-κB downstream of the signaling cascade triggered by IL-1β was investigated. All the

Chart 1. Structures of Reference Compound **1** and Molecules Having the Best Biological Results after Primary Screening (**2**−**6**)

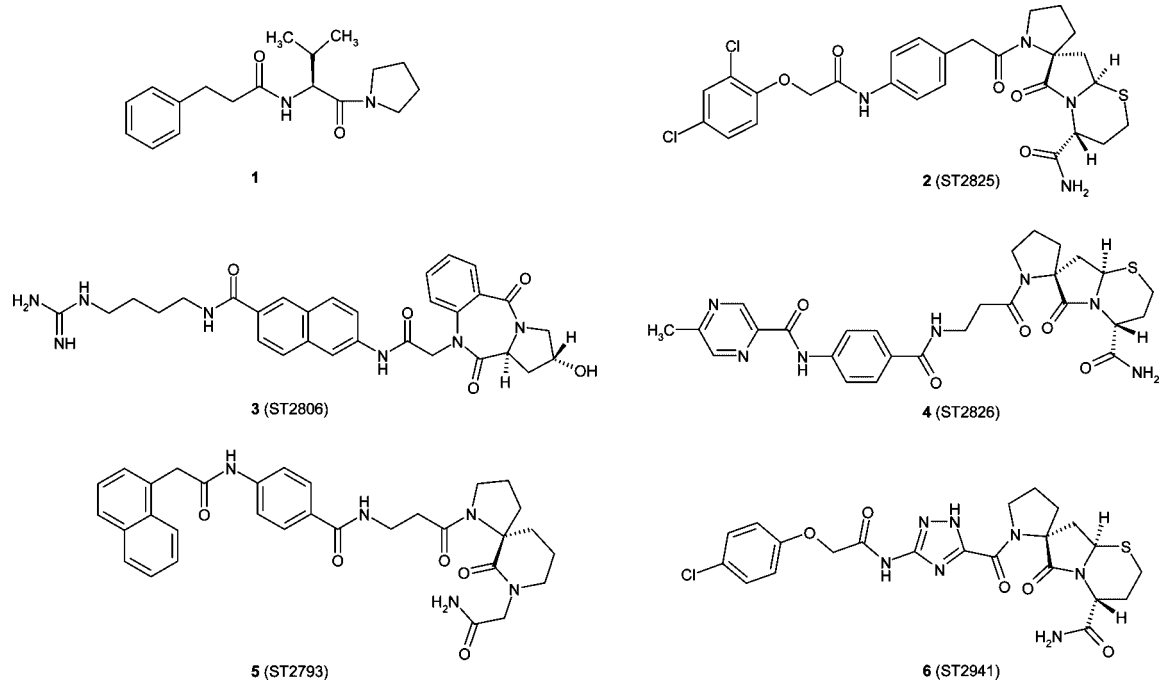

Scheme 1. General Scheme of Parallel SPPS[a]

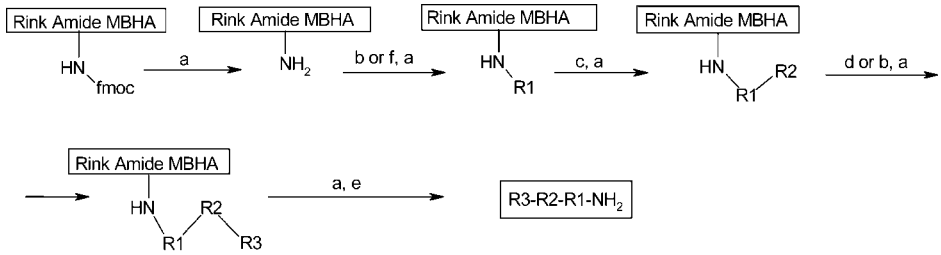

[a] Reagents and conditions: (a) Typical deprotection procedure according to the literature: DMF/CH_2Cl_2, 25% piperidine in DMF, 20 min, rt; (b) Typical procedure for the coupling of β-turn mimetic to the amine group: β-turn mimetic, HOBt/TBTU, DIPEA, DMF, 120 min, rt; (c) Typical procedure for the coupling of a spacer: Fmoc-spacer, HOBt/TBTU, DIPEA, DMF, 120 min, rt; (d) Typical procedure for the coupling of an arginine mimetic group: arginine mimetic, HOBt/TBTU, DIPEA, DMF, 120 min, rt; (e) Typical cleavage procedure: TFA-Tis-H_2O [95:2.5:2.5], 120 min, rt; (f) Typical procedure for the coupling of an arginine mimetic with formation of the guanidine group: Fmoc-isothiocyanate, DMF, 12 h, rt.

Scheme 2. Synthesis of **2**[a]

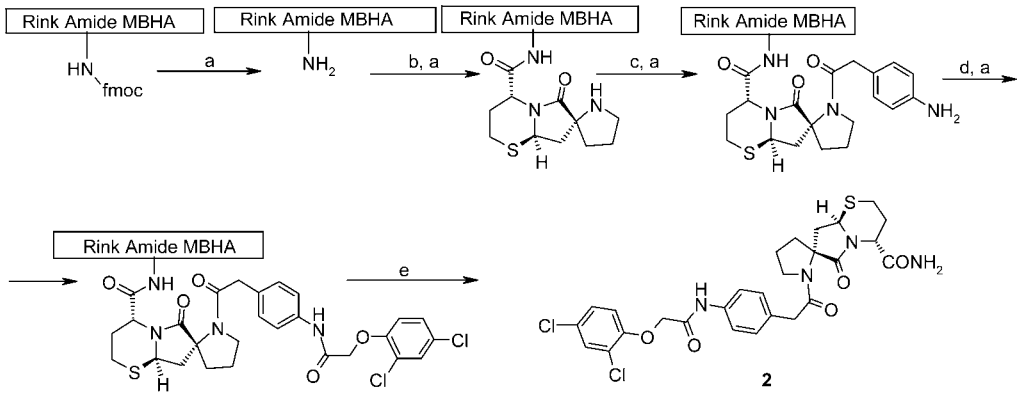

[a] Reagents and conditions: (a) DMF/CH_2Cl_2, 25% piperidine in DMF, 20 min, rt; (b) **18**, HOBt/TBTU, DIPEA, DMF, 120 min, rt; (c) Fmoc-SP19-OH, HOBt/TBTU, DIPEA, DMF, 120 min, rt; (d) PAM4, HOBt/TBTU, DIPEA, DMF, 120 min, rt; (e) TFA-Tis-H_2O [95:2.5:2.5], 120 min, rt.

molecules were concomitantly assayed for cell viability to rule out toxic effects.

Because known inhibitors of MyD88 homodimerization are not yet available, it is not possible to predict how effectively

Scheme 3. Synthesis of **3**[a]

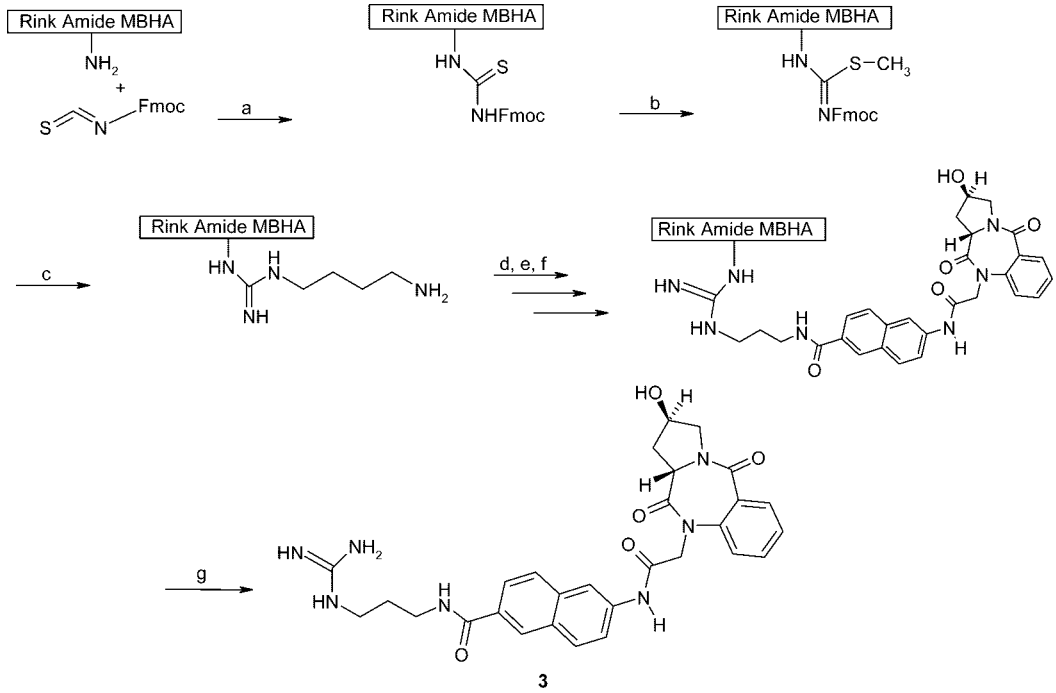

[a] Reagents and conditions: (a) DMF, 12 h, rt; (b) CH_3I/DIPEA, DMF, 2 h, rt; (c) 1,4 diaminobutane, DMF, 12 h, rt; (d) Fmoc-SP38-OH, HOBt/TBTU, DIPEA, DMF, 120 min, rt; (e) TBDPS-O-BETA6-Cl, *sym*-collidine, THF, 70 °C; (f) $Bu_4N^+F^-$, THF, 25 °C; (g) TFA-Tis-H_2O [95:2.5:2.5], 120 min, rt.

the inhibition of MyD88 dimerization translates into the inhibition of IL-1β-induced activation of NF-κB. However, as reference compound in the NF-κB assay, we used a cell-permeable, end-protected L-valyl derivative modeled on the MyD88-binding sequence of the TIR domain BB-loop of IL-1RI; this compound **1** (i.e., hydrocinnamoyl-L-valyl pyrrolidine)[15] was able to specifically inhibit TIR domain-mediated MyD88/IL-1RI interaction, successfully reducing IL-1β-induced fever in mice in vivo and attenuating IL-1β-induced, but not LPS-induced, activation of MAP kinase signaling cascades in murine lymphocytes and EL4 thymoma cells in vitro.

BAY 11-7085, a known pharmacologic inhibitor of IκBα phosphorylation,[18] was used as an additional reference compound in the NF-κB assay. The maximal inhibitory activity observed in our experimental setting was 45% at 10 μM (Table II in Supporting Information).

Chart 1 and Table 4 summarize the structures and positive results in both 2HyS screening and NF-κB assay (expressed as percentage inhibition at 100 μM) obtained with the molecules under investigation and reference compound **1**. In our experimental setting, the inhibitory activities scored by our screened compounds ranged from 17 to 26% (Table 4). Interestingly, the highest activity was shown by **2** (26% inhibition) and was very close to the activity exhibited by Bartfai's compound **1** (31% inhibition at 100 μM).

Moreover, it is worth mentioning that using a different methodology, based on an in-house chemiluminescent NF-κB reporter gene assay, not only were we able to confirm the activity of **2** in vitro, but we further showed that **2** is indeed able to counteract IL-1β signaling in vivo by significantly decreasing IL-1β-dependent production of IL-6 in mice.[19] Interestingly, the doses of **2** utilized in our in vivo study, ranging from 50 to 200 mg/kg, are in the same dose range as those used by Bartfai's compound **1** (namely, 100 mg/kg) in counteracting IL-1β-induced fever in mice.

At variance with Bartfai's inhibitor,[15] which only blocks the interaction between IL-1R and MyD88, the compounds described in the present investigation interfere with MyD88 dimerization, thereby anticipating that they may interfere with signaling from additional TLRs. In fact, we found that **2** effectively inhibited signaling even from ligands operating in an intracellular compartment such as the CpG, that is, the ligand of TLR9, a receptor that depends solely on MyD88 for signal transduction.[19]

The remarkable progress in the elucidation of TLR signaling has elicited great interest from a number of pharmaceutical companies[20] inasmuch as it may lead, in the future, to an entirely new class of therapeutic agents. Indeed, both agonists and antagonists of IL-1R/TLR signaling can find therapeutic application, depending on the clinical setting. Activators may have adjuvant roles, thus improving vaccine efficacy and reinforcing the immune response to cancer,[21] while inhibitors may help dampen inflammation in disorders such as allergy, atherosclerosis, and autoimmune diseases.[22]

SAR Analysis. 2HyS experiments were carried out to assess the ability of the active molecules to specifically interfere with MyD88 homodimerization, while NF-κB assays aimed at testing whether inhibition of MyD88 dimerization translated into inhibition of IL-1β-induced activation of NF-κB. Since both tests are carried out on cell cultures (yeast and mammalian cells), cell membrane/wall permeation, and intrinsic toxicity are strong limiting factors in the selection of positive candidates and in the subsequent SAR analysis.

Nevertheless, some information can be drawn from the present findings on the structure of tested compounds: generally a noncharged arginine mimetic group, a spiro β-turn and a flexible spacer are preferred. The most represented building block is BETA8 (contained in **2**, **4**, and **6**); the characteristic of this β-turn mimetic is a bulky S-containing bicyclic ring linked to natural proline. Activity is enhanced when BETA8 is merged to a *para*-disubstituted six-membered ring. Figure 3 shows the superimposition of compounds in Table 4 and the MyD88 consensus peptide. Noted is a good alignment of the β-turn mimetic skeleton, while unexpectedly bulky hydrophobic groups

Scheme 4. Synthesis of **18**[a]

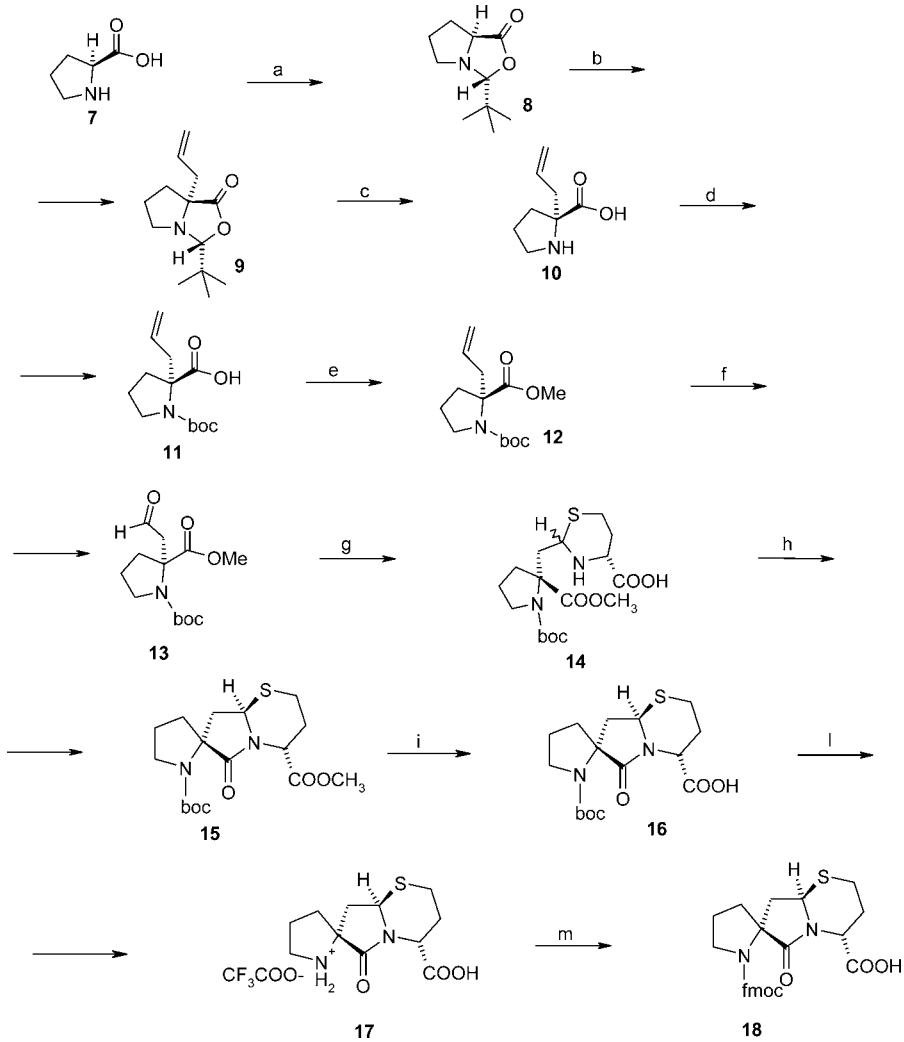

[a] Reagents and conditions: (a) *t*-Bu-CHO, cat. CF_3COOH, *n*-pentane, reflux, 6 d; (b) (1) LDA, THF, –78 °C, 30 min; (2) CH_2=CH-CH_2-Br, 0 °C, 3 h; (c) silica gel, MeOH/H_2O, rt, 72 h; (d) $(Boc)_2O$, $(CH_3)_4N^+OH^-\cdot 5H_2O$, CH_3CN, rt, 72 h; (e) CH_3I, $KHCO_3$, rt, 20 h; (f) OsO_4, $NaIO_4$, MeOH/H_2O, rt, 20 h; (g) D-homocys-OH·HCl, NaOH, H_2O/EtOH, rt, 40 h,; (h) (1) NEt_3, DMF, 70 °C, 3 d; (2) CH_3I, $KHCO_3$, DMF, rt, 24 h; (i) (1) K_2CO_3, MeOH/H_2O, 20 h, rt; (2) pH 5; (l) TFA, rt, 3 h; (m) (1) Fmoc-OSu, $NaHCO_3$, H_2O/$(CH_3)_2CO$, rt, 20 h; (2) HCl 2N, pH 3.

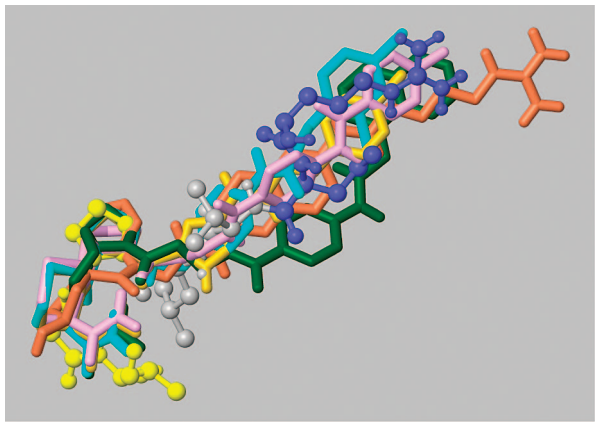

Figure 3. Superimposition of active molecules (*tube*; **2** (cyan), **3** (orange), **4** (pink), **5** (green), and **6** (goldenrod)) onto MyD88 consensus peptide (*ball and stick*; yellow, grey, and blue).

occupy the Gly Cα space; also observed is a preferential agreement on the position of the second amide bond and Asp-Val junction; the arginine mimetic hydrophobic fragment is located on the methylene portion of the Arg side chain.

Table 4. Primary Screening Results

cmpd	composition	2HyS	% NF-κB inhibition
1	hydrocinnamoyl-L-valyl pyrrolidine	n.d.[a]	31
2	PAM4-SP19-BETA8-NH_2	Y	26
3	AM8-SP38-BETA6	Y	24
4	PAM6-SP20-BETA8-NH_2	Y	23
5	PAM8-SP20-BETA3-NH_2	Y	18
6	PAM3-SP33-BETA8-NH_2	Y	17

[a] Not determined.

The listed compounds, with their primary screening results, represent hits that may be further evaluated by investigating their activity in additional and more sensitive functional assays, addressing their effects on cells of the immune system. The most interesting ones may be used as a starting point to generate homologous series aimed at obtaining derivatives with increased inhibitory activity.

Experimental Section

Computational Methods. A virtual library of 4368 direct and 234 retroinverse peptidomimetics was enumerated using TSAR software.[23] The rule of five properties (logP < 5, HBA < 10, HBD < 5, MW < 600, and rotatable bonds < 8) were calculated using TSAR software. EVA descriptors[14] were used to describe the

Scheme 5. Synthesis of **24**[a]

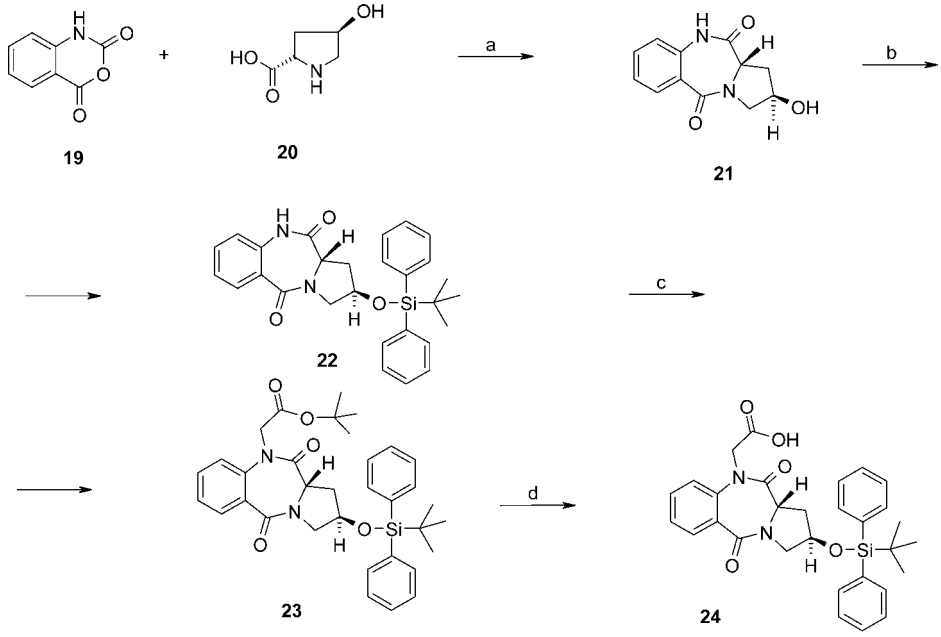

[a] Reagents and conditions: (a) DMSO, 120 °C, 5 h; (b) TBDPSCl, imidazole, DMF, rt, 3.5 h; (c) (1) NaH, –40 °C, 45 min; (2) $BrCH_2COOtBu$, rt, 2 h; (d) CH_2Cl_2/TFA, rt, 45 min.

structures in the experimental design. Principal component analysis was performed on the molecular descriptors matrix using SIMCA-P software.[24] Extracted principal components were processed into MODDE software[25] to perform an onion/D-optimal design.[13]

Chemistry. General Methods. Target compounds described in Chart 1 and Table 4 and all final compounds described in Table 1 of Supporting Information were synthesized on polymer-supported (aminomethyl)polystyrene (Rink amide MBHA, 0.74 mmol/g) with standard 9-fluorenylmethyloxycarbonyl (Fmoc) protocols, using parallel solid-phase peptide synthesis (SPPS) procedures, according to Scheme 1. Single coupling reactions were normally carried out in dimethylformamide (DMF) and 1-hydroxy-1-*H*-benzotriazole/2-(1*H*-benzotriazol-1-yl)-1,1,3,3-tetramethyl-uronium tetrafluoroborate (HOBt-TBTU) was used for chemical activation of the carboxylic component of Fmoc-protected building blocks, while diisopropylethylamine (DIPEA) was used as a proton scavenger. Poor nucleophilic amino peptidyl resins were efficiently coupled, using acid chlorides of corresponding building blocks at 70 °C for 2 h in tetrahydrofuran (THF) in the presence of *sym*-collidine. Fmoc-protected amino acids, solvents, and reagents were purchased from Chem-Impex, while Rink amide MBHA resin and unprotected amino benzoic derivatives (spacers) were supplied by Sigma-Aldrich. The amine function of the benzoic derivatives was protected by Fmoc according to methods described in the literature.[26a] Target compounds were characterized by mass spectrometry and purity was determined by analytical HPLC on Thermofinnigan LCQ-Duo with adjustable API-ESI ion source, using a gradient system composed of solvent (A) H_2O + 0.1% TFA and (B) MeCN + 0.1% TFA from 95 to 40% solvent (A) in 13 min; Phenomenex Luna RP-C18 column, 3 μm, 50 × 2 mm; flow rate 0.5 mL/min. Semipreparative HPLC purifications of target compounds were performed on Labservice Analitica Labflow 2000 and 3000 with a Knauer K-2501 UV detector and with a Phenomenex Jupiter-Proteo RP-C12 column, 250 × 21.2 mm, 10 μm, 90 Å; using a gradient system composed of solvent (A) H_2O/MeCN/TFA 97/3/0.1 and solvent (B) MeCN/H_2O/TFA 80/20/0.1 from 95 to 40% solvent (A) in 30 min; flow rate 15 mL/min. NMR spectra of intermediate compounds were obtained on a Varian VXR 300 and spectra elaboration was performed by standard Varian software (VNMR, 6.1C release); chemical shifts are reported in parts per million (ppm) using the middle resonance of D_2O, $CDCl_3$, or MeOH-d_4 as an internal standard. NMR spectra of target compounds were obtained at 27 °C on a Varian Inova-500 equipped with a triple resonance indirect probe operating at 500.0 MHz for ^1H and 125.67 MHz for ^{13}C (Varian). Data acquisition, Fourier transformation, and spectra elaboration were performed by standard Varian software (VNMR, 6.1C release); chemical shifts are reported in parts per million (ppm) using the middle resonance of DMSO-d_6 or MeOH-d_4 as an internal standard. About 5 mg of all samples were dissolved in DMSO-d_6 or MeOH-d_4 (Sigma-Aldrich) and extensively analyzed by means of 2D-NMR spectroscopy ($^1H-^1H$ COSY, $^1H-^{13}C$ gs-HSQC, $^1H-^{13}C$ gs-HMBC). The following abbreviations are used to describe peak patterns when appropriate: b = broad, s = singlet, d = doublet, dd = double–doublet, dt = double triplet, t = triplet, q = quartet, m = multiplet. Intermediate compounds were characterized by mass spectrometry on Single Quadrupole Micromass Waters ZQ2000 mass spectrometer with ESI ion source. Melting points were obtained in open capillary tubes and are uncorrected. Thin layer chromatography (TLC) was carried out on Merck precoated plates (Kieselgel 60F254), and compounds were visualized using a UV lamp at 254 and 366 nm. Elemental analyses were performed on a Thermo EA1110 CHNS-O instrument. Reference compound **1** (i.e., hydrocinnamoyl-L-valyl pyrrolidine) was prepared according to the literature.[15]

Synthesis of (2*R*,4′*R*,8a′*R*)-1-[(9*H*-Fluoren-9-yl-methoxy)carbonyl]-6′-oxotetrahydro-2′*H*-spiro[pyrrolidine-2,7′-pyrrole-[2,1-*b*][1,3]thiazine]-4′-carboxylic Acid, Fmoc-BETA8-OH (18): **(3*S*,7a*S*)-3-*tert*-Butyltetrahydro-1*H*-pyrrolo[1,2-*c*][1,3]oxazol-1-one (8).** Compound **8** was prepared according to the literature (yield 80%).[11a] Bp 84–85 °C (0.05 mm). ^1H NMR (300 MHz, $CDCl_3$): δ 0.92 (s, 9H), 1.60–1.92 (m, 2H), 1.94–2.30 (m, 2H), 2.64–2.98 (m, 1H), 3.05–3.35 (m, 1H), 3.80 (dd, 1H), 4.50 (s, 1H).

(3*S*,7a*R*)-7a-Allyl-3-*tert*-butyltetrahydro-1*H*-pyrrolo[1,2-*c*][1,3]oxazol-1-one (9). Compound **9** was prepared according to the literature (yield 75%).[11a] Bp 80–82 °C (0.01 mm). TLC solvents: *n*-hexane/AcOEt 8/2, R_f 0.72. ^1H NMR (300 MHz, $CDCl_3$): δ 0.87 (s, 9H), 2.14–1.34 (m, 4H), 2.35 (d, 2H), 3.05–2.70 (m, 2H), 4.20 (s, 1H), 5.24–4.90, 6.14–5.60 (m, 3H).

(*R*)-2-Allyl-proline (10). Compound **10** was prepared according to the literature (yield 70%).[11b] $[\alpha]^{20}_D$ = –46.3 (*c* 0.5, H_2O). ^1H NMR (300 MHz, D_2O): δ 2.00 (m, 3H), 2.04 (m, 1H), 2.58 (dd, 1H), 2.90 (dd, 1H), 3.45 (m, 2H), 5.25 (s, 1H), 5.32 (d, 1H), 5.65–5.90 (m, 1H). ESIMS *m*/*z* 156.2 $(M + H)^+$.

Scheme 6. Synthesis of **33**[a]

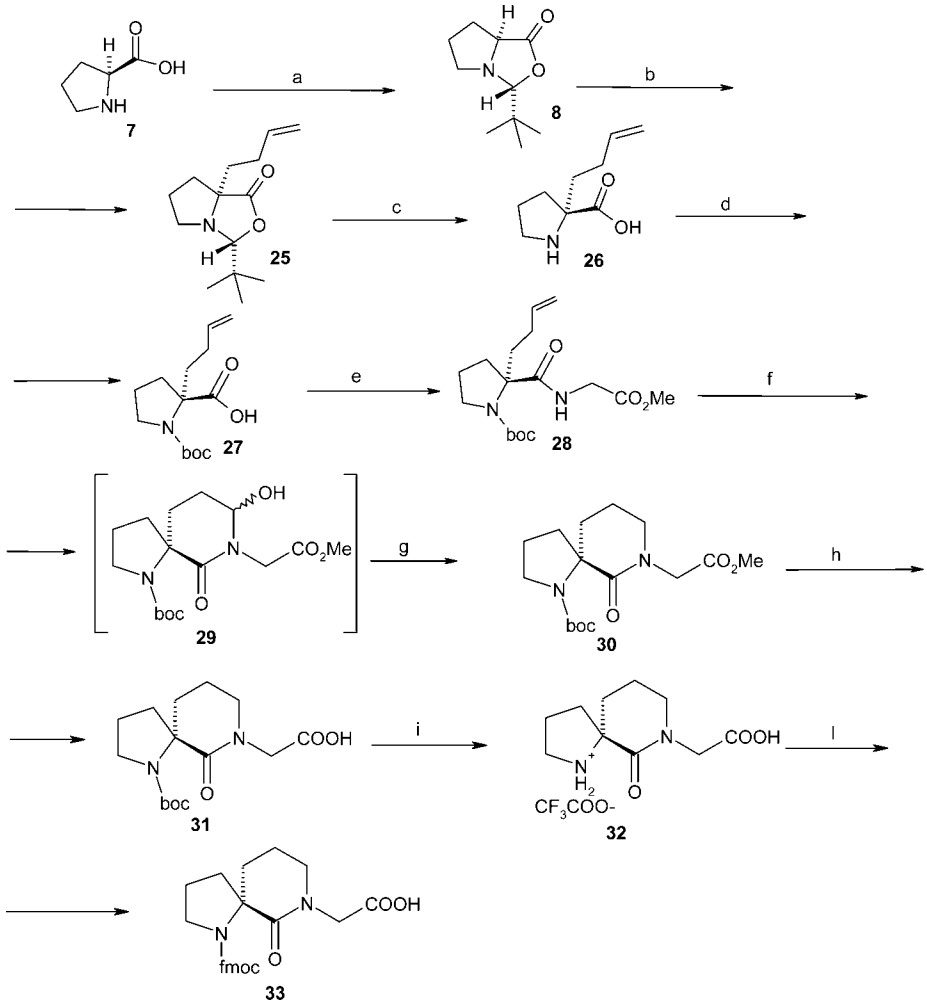

[a] Reagents and conditions: (a) *t*-Bu-CHO, cat. TFA, *n*-pentane, reflux, 6 d; (b) (1) LDA, THF/DMPU, –78 °C, 1 h; (2) CH_2═CH-CH_2-CH_2-Br, –78 °C, 20 h; (c) silica gel, MeOH/H_2O, rt, 72 h; (d) $(Boc)_2O$, $(CH_3)_4N^+OH^-\cdot 5H_2O$, rt, 72 h; (e) Gly OMe·HCl, DCC, HOBt, NEt_3, $CHCl_3$, N_2, rt, 20 h; (f) OsO_4, N_2, $NaIO_4$, MeOH/H_2O, rt, 24 h; (g) $NaBH_3CN$, THF/TFA, N_2, rt, 20 h; (h) (1) K_2CO_3, MeOH/H_2O, rt, 20 h; (2) HCl, pH 2−3; (i) TFA/CH_2Cl_2, rt, 1 h; (l) (1) Fmoc-OSu, $NaHCO_3$, H_2O/$(CH_3)_2CO$, rt, 24 h; (2) HCl 2 N, pH 2–3.

(*R*)-2-Allyl-*N*-(*tert*-butoxycarbonyl)-proline (11). Compound **11** was prepared according to the literature (yield 85%).[11c] $[\alpha]^{20}_D$ = +58.4 (*c* 1.2, MeOH). ^{1}H NMR (300 MHz, $CDCl_3$): δ 1.40, 1.45 (s, 9H), 1.75–1.94 (m, 2H), 1.98–2.02, 2.35–2.40 (m, 1H), 2.12–2.16 (m, 1H), 2.58 (dd, 1H), 2.95 (dd, 1H), 3.28–3.40 (m, 1H), 3.50–3.70 (m, 1H), 5.10–5.18 (m, 2H), 5.62–5.82 (m, 1H), 10.90 (bs, 1H). ESIMS *m*/*z* 256.3 $(M + H)^+$.

(*R*)-2-Allyl-*N*-(*tert*-butoxycarbonyl)-proline Methyl Ester (12). Compound **12** was prepared according to the literature (yield 95%).[11c] $[\alpha]^{20}_D$ = +49.6 (*c* 0.9, MeOH). ^{1}H NMR (300 MHz, $CDCl_3$): δ 1.40, 1.45 (s, 9H), 1.76–1.93 (m, 2H), 2.02–2.16 (m, 2H), 2.58 (dd, 1H), 2.95, 3.10 (dd, 1H), 3.30–3.40 (m, 1H), 3.55–3.70 (m, 1H), 3.72 (s, 3H), 5.10–5.15 (m, 2H), 5.72–5.78 (m, 1H). ESIMS *m*/*z* 292.4 $(M + Na)^+$.

(2*R*)-2-(2-Oxoethyl)pyrrolidine-1,2-dicarboxylic Acid 1-*tert*-Butyl 2-Methyl Ester (13). Compound **13** was prepared according to the literature (yield 80%).[11c] $[\alpha]^{20}_D$ = +136.7 (*c* 1.0, $CHCl_3$). ^{1}H NMR (300 MHz, $CDCl_3$): δ 1.38, 1.40 (s, 9H), 1.80–2.00 (m, 2H), 2.14–2.28 (m, 2H), 2.70–3.09 (m, 2H), 3.42–3.78 (m, 2H), 3.70, 3.72 (s, 3H), 9.77, 9.78 (s, 1H). ESIMS *m*/*z* 294.4 $(M + Na)^+$.

(4*R*)-2-{[(2*R*)-1-(*tert*-Butoxycarbonyl)-2-(methoxycarbonyl)pyrrolidin-2-yl]methyl}-1,3-thiazinane-4-carboxylic Acid (14). Compound **14** was prepared according to the literature (yield 65%).[11c] Mp 90–95 °C (lit.[11c] mp 94–97 °C). ^{1}H NMR (300 MHz, $CDCl_3$): δ 1.46 (s, 9H), 1.75–2.20 (m, 4H), 2.15–2.82 (m, 4H), 2.82–3.15 (m, 2H), 3.18–4.62 (m, 3H), 4.78 (s, 3H), 4.20, 4.34 (s, 1H). ESIMS *m*/*z* 389.5 $(M + H)^+$.

(2*R*,4′*R*,8a′*R*)-6′-Oxotetrahydro-1*H*,2′*H*-spiro[pyrrolidine-2,7′-pyrrolo[2,1-*b*][1,3]thiazine]-1,4′-dicarboxylic acid 1-*tert*-Butyl 4′-Methyl Ester (15). Compound **15** was prepared according to the literature (yield 40%).[11c] Mp 152–154 °C (lit.[11c] mp 156–158 °C). $[\alpha]^{20}_D$ = +129.6 (*c* 1.2, $CHCl_3$). ^{1}H NMR (300 MHz, $CDCl_3$): δ 1.39, 1.42 (s, 9H), 1.70–2.10 (m, 4H), 2.10–2.40 (m, 3H), 2.62 (dt, 1H), 2.82 (dd, 1H), 2.90–3.10 (m, 1H), 3.40–3.60 (m, 2H), 3.76, 3.79 (s, 3H), 5.05–5.18 (m, 1H), 5.32, 5.43 (d, 1H). ESIMS *m*/*z* 393.3 $(M + Na)^+$.

(2*R*,4′*R*,8a′*R*)-1-(*tert*-Butoxy-carbonyl)-6′-oxotetrahydro-2′*H*-spiro[pyrrolidine-2,7′-pyrrole[2,1-*b*]-[1,3]-thiazine]-4′-carboxylic Acid (16). (2*R*,4′*R*,8a′*R*)-6′-Oxotetrahydro-1*H*,2′*H*-spiro[pyrrolidine-2,7′-pyrrole[2,1-*b*][1,3]thiazine]-1,4′-dicarboxylic acid 1-*tert*-butyl 4′-methyl ester **15** (2.55 g, 6.9 mmol) was dissolved in 45 mL of MeOH and 45 mL of H_2O; K_2CO_3 (1.9 g, 13.8 mmol) was added to the solution and kept under stirring at room temperature for 20 h, then treated by lowering the pH to 5, bringing to dryness under reduced pressure. The residue obtained was collected with H_2O, brought to pH 2–3 and extracted with $CHCl_3$. The organic phase was dried over anhydrous Na_2SO_4 and the solvent was evaporated. The pitchy mass was crystallized with ethyl ether, thereby obtaining a filterable white solid (2.4 g, 97%). TLC solvents: $CHCl_3$/MeOH/CH_3COOH 7.95/1.95/0.1, R_f 0.65. ^{1}H NMR (300 MHz, $CDCl_3$)δ 1.40, 1.45 (2d, 9H), 2.70–2.05 (m, 4H), 2.00–2.30 (m, 1H), 2.25–2.55 (m, 1H), 2.55–2.80 (m, 1H), 2.75–3.15 (m, 1H), 3.50 (m, 2H), 3.70 (t, 2H), 4.98 (dd, 1H), 5.10 (d, 1H). ESIMS *m*/*z* 379.3 $(M + Na)^+$.

(2*R*,4′*R*,8a′*R*)-4′-Carboxy-6′-oxotetrahydro-2′*H*-spiro[pyrrolidine-2,7′-pyrrole[2,1-*b*][1,3]thiazine] Trifluoroacetate (17). (2*R*,4′*R*,8a′*R*)-1-(*tert*-Butoxycarbonyl)-6′-oxotetrahydro-2′*H*-spiro[pyrrolidine-2,7′-pyrrole[2,1-*b*][1,3]thiazine]-4′-carboxylic acid **16** (2.1 g, 5.8 mmol) was dissolved in 45 mL of trifluoroacetic acid. The mixture was kept under stirring at room temperature for 3 h and evaporated to dryness at 30 °C under reduced pressure. The residue obtained was solubilized in a small amount of $CHCl_3$, precipitated with ethyl ether, and the solid formed was rapidly filtered. This step was performed twice, obtaining a very hygroscopic white solid (1.55 g, 74%). TLC solvents: $CHCl_3$/isoPrOH/MeOH/H_2O/AcOH 4.2/0.7/2.8/1.05/1.05, R_f 0.56. ^{1}H NMR (300 MHz, D_2O): δ 1.75–2.00 (m, 1H), 2.00–2.38 (m, 5H), 2.45 (dd, 1H), 2.70 (dt, 1H), 2.77–3.05 (m, 2H), 3.25–3.55 (m 2H), 3.96 (d, 1H), 5.18 (d, 1H). ESIMS *m*/*z* 258.3 $(M + H)^+$.

(2*R*,4′*R*,8a′*R*)-1-[(9*H*-Fluoren-9-yl-methoxy)carbonyl]-6′-oxotetrahydro-2′*H*-spiro[pyrrolidine-2,7′-pyrrole-[2,1-*b*][1,3]thiazine]-4′-carboxylic Acid (18). (2*R*,4′*R*,8a′*R*)-4′-Carboxy-6′-oxotetrahydro-2′*H*-spiro[pyrollidine-2,7′-pyrrole[2,1-*b*]-[1,3]thiazine] Trifluoroacetate **17** (1.48 g, 4.0 mmol) was dissolved in 50 mL of H_2O. $NaHCO_3$ (0.67 g, 8.0 mol) was added to the solution followed by 1.42 g (4.2 mmol) of Fmoc-*N*-OSu dissolved in 75 mL of acetone. The reaction solution was left under stirring at room temperature for 20 h, eliminating the acetone under reduced pressure. H_2O was added and the solution was washed with Et_2O. The aqueous solution was brought to pH 3 with HCl 2N and extracted with $CHCl_3$. The organic phase was dried over anhydrous Na_2SO_4 and the solvent was evaporated, obtaining a glassy white solid (1.9 g, 98%). TLC solvents: $CHCl_3$/MeOH/AcOH 7.95/1.95/0.1, R_f 0.74. Mp 108–115 °C. $[\alpha]^{20}_D = +70.1$ (*c* 0.5, MeOH). ^{1}H NMR (300 MHz, $CDCl_3$): δ 1.85 (m, 1H), 1.94 (dd, 1H), 2.05 (m, 1H), 2.15 (m, 1H), 2.42 (m, 1H), 2.67 (d, 1H), 2.82 (m, 2H), 3.00 (m, 1H), 3.58 (dd, 2H), 4.20 (t, 1H). HPLC: column, Symmetry C18 (5μ) 3.9 × 150 mm; mobile phase, KH_2PO_4 50 mM/CH_3CN 65/35; flow rate, 1.0 mL/min; RT, 12.19 min. ESIMS *m*/*z* 501.3 $(M + Na)^+$. Anal. ($C_{26}H_{26}N_2O_5S \cdot 2H_2O$) C, H, N. C: calcd, 60.70; found, 56.77. H: calcd, 5.84; found, 4.85. N: calcd, 5.45; found, 5.06. S: calcd, 6.23; found, 5.26.

SPPS Synthesis of (2*R*,4′*R*,8a′*R*)-1-[(4-{[(2,4-Dichlorophenoxy)-acetyl]amino}phenyl) acetyl]-6′-oxotetrahydro-2′*H*-spiro[pyrrolidine-2,7′-pyrrolo[2,1-*b*][1,3]thiazine]-4′-carboxamide, AM4-SP19-BETA8-NH$_2$ (2). Step 1: Attachment of β-Turn Mimetic 14 to Rink Amide MBHA. Typical Procedure. Compound **18** (250 μmol, 116 mg), prepared according to Scheme 4, was dissolved in a 1.0 M solution of DIPEA in DMF (0.5 mL) and a 0.5 M solution of HOBt-TBTU in DMF (0.5 mL). The mixture was added to Rink amide MBHA resin, previously treated for Fmoc removal (66 mg, ∼50 μmol). The suspension was shaken for 2 h, filtered off, and, after washing with DMF, the resin was allowed to react for 20 min with a 25% piperidine solution in DMF (1 mL) for Fmoc removal. After washing, the resin was used for the subsequent step.

Step 2: Attachment of Spacer (Fmoc-SP19-OH) to H-β-Turn Mimetic-Rink Amide MBHA Resin (H-BETA8-Rink Amide Resin). Typical Procedure. Fmoc-SP19-OH (250 μmol, 94 mg), dissolved in a 1.0 M solution of DIPEA in DMF (0.5 mL) and a 0.5 M solution of HOBt-TBTU in DMF (0.5 mL), was added to BETA8-Rink amide MBHA resin. The suspension was gently shaken for 2 h, filtered off, washed, and then the resin was allowed to react for Fmoc removal, as described in Step 1. Then the resin was dried with a nitrogen flow and used for the subsequent step.

Step 3: Attachment of Arginine Mimetic (PAM4) to H-Spacer-β-Turn Mimetic-Rink Amide MBHA Resin (H-SP19-BETA8-Rink Amide Resin). Typical Procedure. To the pseudoeptidyl resin from Step 2, suspended in THF (1.0 mL) in a glass reactor with a screw cap, was added *sym*-collidine (500 μL) and acid chloride of PAM4 (250 μmol), then shaking for 2 h at 70 °C. Subsequently, the resin was filtered off, washed, dried, and allowed to react to get cleavage of the peptidomimetic sequence.

Step 4: Cleavage of Sequence from the Resin. Typical Procedure. The dry resin from the previous step was treated with a mixture of TFA/triisopropylsilane/H_2O (TFA-Tis-H_2O) 95:2,5:2.5 (1.0 mL). The reaction was shaken for 2 h and then filtered off. The solution, evaporated under reduced pressure, yielded a residue which, after RP-HPLC purification, provided pure **2** (9.3 mg, 29%); analytical HPLC showed a peak related to the product at 12.28 min, purity > 93%. Mass value in agreement with theoretical value: ESIMS *m*/*z* 591.04 $(M + H)^+$, 613.18 $(M + Na)^+$. ^{1}H NMR (Figure I of the Supporting Information reports the numbering system used for the attribution of main signals, 500 MHz, DMSO-d_6): δ 1.52–1.64 (m, 1H, 3-CH″), 1.86–1.98 (m, 3H, 7-CH″,11-CH″, 12-CH″), 1.98–2.13 (m, 2H, 11-CH″, 12-CH″), 2.53–2.57 (m, 1H, 3-CH″), 2.61–2.83 (m, 3H, 2-CH_2, 7-CH″), 3.41–3.53 (m, 1H, 10-CH″), 3.64 (s, 2H, 20-CH_2), 3.66 (d, J = 7.9 Hz, 1H, 10-CH″), 4.61 (d, J = 4.6 Hz, 1H, 4-CH), 4.85 (s, 2H, 30-CH_2), 4.97 (dd, J = 7.6, 1.6 Hz, 1H, 6-CH), 7.11 (d, J = 8.9 Hz, 1 H, 37-CH), 7.17 (d, J = 8.2 Hz, 2H, 22-CH, 26-CH), 7.21 (bs, 1H, 19-NH′), 7.38 (dd, J = 8.9, 1.8 Hz, 1H, 36-CH), 7.50 (bs, 1H, 19-NH″), 7.53 (d, J = 8.2 Hz, 2H, 23-CH, 25-CH), 7.61 (d, J = 1.8 Hz, 1H, 34-CH), 10.14 (s, 1H, 27-NH); ^{13}C NMR (125.67 MHz, DMSO-d_6): δ 24.48 (11-C), 25.59 (3-C), 26.02 (2-C), 37.91 (7-C), 38.46 (12-C), 41.20 (20-C), 48.63 (10-C), 52.07 (4-C), 55.04 (6-C), 66.39 (8-C), 68.60 (30-C), 116.04 (37-C), 120.20 (23-C, 25-C), 123.21 (33-C), 125.75 (35-C), 128.74 (36-C), 130.05 (22-C, 26-C), 130.09 (34-C), 130.81 (21-C), 137.49 (24-C), 153.37 (32-C), 166.26 (28-C), 169.84 (16-C), 170.80 (14-C), 172.61 (13-C).

Synthesis of [(2*R*,11a*S*)-2-{[*tert*-Butyl(diphenyl)silyl]oxy}-5,11-dioxo-2,3,11,11a-tetrahydro-1*H*-pyrrole[2,1-*c*][1,4]benzodiazepine-10(5*H*)-yl]-acetic Acid, TBDPS-O-BETA6 (24): (2*R*,11a*S*)-2-Hydroxy-2,3-dihydro-1*H*-pyrrole[2,1-*c*][1,4]benzodiazepine-5,11(10-*H*,11a*H*)-dione (21). Compound **21** was prepared according to the literature (yield 80%).[10] TLC solvent AcOEt R_f 0.3, mp 200–202 °C (lit.[10] mp 198–200 °C). $[\alpha]^{20}_D = +410.2$ (*c* 0.02, MeOH). ^{1}H NMR (300 MHz, DMSO-d_6): δ 1.92 (m, 1H), 2.61 (m, 1H), 3.50 (m, 1H), 3.62 (dd, 1H), 4.22 (dd, 1H), 4.32 (m, 1H), 5.23 (d, 1H), 7.16 (d, 1H), 7.23 (t, 1H), 7.53 (m, 1H), 7.82 (dd, 1H), 10.55 (s, 1H). ESIMS *m*/*z* 255.2 $(M + Na)^+$. Anal. ($C_{12}H_{12}N_2O_3$) C, H, N. C: calcd, 62.06; found, 61.90; H: calcd, 5.21; found, 5.18; N: calcd, 12.06; found, 11.98.

(2*R*,11a*S*)-2-{[*tert*-Butyl(diphenyl)-silyl]oxy}-2,3-dihydro-1*H*-pyrrole[2,1-*c*][1,4]benzo diazepine-5,11(10-*H*,11a*H*)-dione (22). (2*R*,11a*S*)-2-Hydroxy-2,3-dihydro-1*H*-pyrrole[2,1-*c*][1,4]benzodiazepine-5,11(10*H*,11a*H*)-dione **21** (2.3 g, 10.0 mmol) was dissolved in 30 mL of DMF; then imidazole (3.4 g, 50.0 mmol) and also 5.6 mL (22.0 mmol) of *tert*-butyl-diphenyl-silylchloride were added to this solution dropwise under stirring. The solution was kept under stirring at room temperature for 3.5 h, and then 100 mL of H_2O were added; for extraction, 100 mL of CH_2Cl_2 were used, washing the organic phase with H_2O. The organic phase was dried over anhydrous Na_2SO_4, and the solvent was evaporated under reduced pressure using a mechanical pump, obtaining a dense oil that was solubilized hot in *n*-hexane/AcOEt and reprecipitated several times. After drying with the mechanical pump, an amorphous solid was obtained (3.9 g, 83%). TLC solvents: *n*-hexane/AcOEt 6/4, R_f 0.5. ^{1}H NMR (300 MHz, $CDCl_3$): δ 1.03 (s, 9H), 2.20 (m, 1H), 2.78 (m, 1H), 3.55, 3.60 (2d, 1H), 3.85, 3.90 (2d, 1H), 4.25 (m, 1H), 4.55 (m, 1H), 7.00 (d, 1H), 7.25–7.55 (m, 8H), 7.60–7.80 (m, 4H), 8.02 (d, 1H), 8.65 (s, 1H). ESIMS *m*/*z* 493.6 $(M + Na)^+$. Anal. ($C_{28}H_{30}N_2O_3Si$) C, H, N. C: calcd, 71.45; found, 70.47; H: calcd, 6.42; found, 6.67; N: calcd, 5.95; found, 5.53.

[(2*R*,11a*S*)-2-{[*tert*-Butyl-(diphenyl)silyl]oxy}-5,11-dioxo-2,3,11,11a-tetrahydro-1*H*-pyrrole-[2,1-*c*]-[1,4]benzodiazepine-10(5*H*)-yl)-acetic Acid *tert*-Butyl Ester (23). NaH 60% (330 mg, 8.0 mmol) was suspended in 6 mL of anhydrous THF after washing several times with THF. The suspension was cooled to –40 °C and (2*R*,11a*S*)-2-{[*tert*-butyl(diphenyl)-silyl]oxy}-2,3-dihydro-1*H*-pyrrole[2,1-*c*][1,4]benzodiazepine-5,11(10*H*, 11a*H*)-dione **22** (3.45 g, 7.3 mmol), dissolved in 18 mL of THF, was added dropwise, maintaining the solution under stirring. After 45 min, *tert*-butyl-bromoacetate (1.2 mL, 8.0 mmol) was added dropwise, and the mixture was left to react under stirring for 2 h, allowing the

temperature to rise to room temperature. The suspension was then poured into 50 mL of H_2O and extracted twice with 30 mL of CH_2Cl_2, washing the pooled organic phases several times with brine and dried over anhydrous Na_2SO_4. The solution was evaporated under reduced pressure, obtaining an oil that, after repeated washing with petroleum ether and drying with a mechanical pump, gave an amorphous solid (3.6 g, 84%). TLC solvents: *n*-hexane/AcOEt 7/3, R_f 0.5. ^{1}H NMR (300 MHz, $CDCl_3$): δ 1.03 (s, 9H), 1.45 (s, 9H), 2.15 (m, 1H), 2.80 (m, 1H), 3.55, 3.60 (2d, 1H), 3.75, 3.82 (2d, 1H), 4.30 (m, 1H), 4.05–4.60 (dd, 2H), 4.62 (m, 1H), 7.20 (d, 1H), 7.30–7.60 (m, 8H), 7.60–7.80 (m, 4H), 8.00 (d, 1H); ESIMS *m*/*z* 607.5 $(M + Na)^+$. Anal. ($C_{34}H_{40}N_2O_5Si$) C, H, N. C: calcd, 69.83; found, 68.87; H: calcd, 6.89; found, 7.37; N: calcd, 4.79; found, 4.01.

[(2*R*,11a*S*)-2-{[*tert*-Butyl(diphenyl)silyl]oxy}-5,11-dioxo-2,3,11,11a-tetrahydro-1*H*-pyrrole[2,1-*c*][1,4]benzodiazepine-10(5*H*)-yl]-acetic Acid (24). [(2*R*,11a*S*)-2-{[*tert*-butyl-(diphenyl)silyl]oxy}-5,11-dioxo-2,3,11,11a-tetrahydro-1*H*-pyrrole[2,1-*c*]-[1,4]benzo diazepine-10(5*H*)-yl)-acetic acid *tert*-butyl ester **23** (3.6 g, 6.1 mol) was suspended in 30 mL of CH_2Cl_2, and 25 mL of trifluoroacetic acid were added dropwise, under stirring, at 15 °C. The temperature was allowed to rise to room temperature, and the solution was left under stirring for 45 min. The reaction solution was brought to dryness under reduced pressure with a mechanical pump, and the residue was solubilized in ethyl ether from which it was precipitated by cooling, yielding a white solid (2.6 g, 81%). TLC solvents: $CHCl_3$/MeOH 7/3, R_f 0.7; mp 191–193 °C. $[\alpha]^{20}_D$ = +246.2 (*c* 1.0, $CHCl_3$). HPLC: Inertsil ODS 3 column (5μ), 4.6 × 250 mm; mobile phase, CH_3CN/KH_2PO_4 50 mM 70/30; pH 3 (H_2PO_4 85%); flow rate, 1.0 mL/min, t = 30 °C; RT, 10.79 min. ^{1}H NMR (300 MHz, $CDCl_3$): δ 1.03 (s, 9H), 2.05 (m, 1H), 2.75 (m, 1H), 3.50, 3.55 (2d, 1H), 3.75, 3.78 (2d, 1H), 4.25 (m, 1H), 4.20–4.57 (dd, 2H), 4.60 (m, 1H), 7.10 (d, 1H), 7.20–7.50 (m, 8H), 7.60 (m, 4H), 7.90 (d, 1H). ESIMS *m*/*z* 551.2 $(M + Na)^+$. Anal. ($C_{30}H_{32}N_2O_5Si$) C, H, N. C: calcd, 68.16; found, 67.12; H: calcd, 6.10; found, 6.09; N: calcd, 5.30; found, 5.28.

SPPS Synthesis of *N*-(4-{[Amino(imino)methyl]amino}butyl)-6-({[(2*R*,11a*S*)-2-hydroxy-5,11-dioxo-2,3,11,11a-tetrahydro-1*H*-pyrrolo[2,1-*c*][1,4]benzodiazepin-10(5*H*)-yl]acetyl}amino)-2-naphthamide, AM8-SP38-BETA6 (3). Typical Procedure for the Coupling of an Arginine Mimetic with Formation of the Guanidine Group. Fmoc-isothiocyanate (0.5 mmol) in DMF (2.0 mL) was added to Rink amide MBHA resin (66 mg, ~50 μmol) free of Fmoc protecting group. The suspension was shaken for 12 h, filtered off, washed with DMF, and reacted with a solution of CH_3I (10 equiv relative to the resin) and DIPEA (30 equiv relative to the resin) in DMF (3.0 mL). The mixture was shaken for 2 h at room temperature, filtered off, and washed with DMF. Then 2-methyl-isothioureyl-resin was added, recovered from the previous reaction, to a solution of 1,4-diaminobutane (10 equiv relative to the resin) in DMF (2.0 mL) and shaken for 12 h at room temperature. Afterward, the resin was filtered off and washed with DMF.

Synthesis was then accomplished following the typical procedures described in Steps 1 and 3 of SPPS synthesis of **2**, using Fmoc-SP38-OH (250 μmol) and *tert*-butyldiphenylsilyl-O-BETA6 acid chloride (TBDPS-O-BETA6-Cl; 250 μmol), prepared using **24** (Scheme 5) by treatment with thionyl chloride and cleavage of the TBDS protective group with $Bu_4N^+F^-$, as previously described.[26b] Cleavage from the resin, as described in Step 4 of the SPPS synthesis of **2**, and RP-HPLC purification of crude product gave **3** (0.9 mg, 2.85%); analytical HPLC showed a peak related to the product at 6.78 min, purity > 90%. Mass value agrees with theoretical value: ESIMS *m*/*z* 572.33 $(M + H)^+$. ^{1}H NMR (Figure I of Supporting Information reports numbering system used for the attribution of main signals, 500 MHz, MeOH-d_4): δ 1.64–1.80 (m, 4 H, 36-CH_2, 37-CH_2), 2.08–2.17 (m, 1 H, 4-CH″), 2.86–2.96 (m, 1H, 4-CH″), 3.28 (t, J = 6.9 Hz, 2H, 38-CH_2), 3.50 (t, J = 6.0 Hz, 2H, 35-CH_2), 3.69 (dd, J = 12.2, 4.7 Hz, 1H, 2-CH″), 3.77 (dd, J = 12.2, 2.7 Hz, 1H, 2-CH″), 4.45 (t, J = 6.0 Hz, 1H, 5-CH), 4.55–4.60 (m, 1H, 3-CH), 4.64 (d, J = 16.7 Hz, 1H, 17-CH″), 4.84 (d, J = 16.7 Hz, 1H, 17-CH″), 7.43 (t, J = 7.6 Hz, 1H, 13-CH), 7.54 (d, J = 8.4 Hz, 1H, 11-CH), 7.68 (t, 1H, 12-CH), 7.69 (d, 1H, 23-CH), 7.84–7.92 (m, 3H, 14-CH, 28-CH, 29-CH), 7.96 (d, J = 9.1 Hz, 1H, 24-CH), 8.34 (bs, 2H, 26-CH, 31-CH); ^{13}C NMR (125.67 MHz, MeOH-d_4): δ 26.06 (37-C), 26.71 (36-C), 34.61 (4-C), 39.09 (35-C), 41.00 (38-C), 52.93 (17-C), 53.66 (2-C), 56.27 (5-C), 68.63 (3-C), 116.10 (31-C), 120.75 (23-C), 122.87 (11-C), 124.25 (29-C), 126.17 (13-C), 127.33 (26-C), 127.79 (28-C), 129.26 (9-C), 129.67 (24-C), 129.74 (14-C), 129.90 (25-C), 130.72 (30-C), 132.76 (12-C), 135.65 (27-C), 137.81 (22-C), 140.38 (8-C), 157.51 (40-C), 166.80 (10-C), 167.78 (18-C), 169.19 (32-C), 169.88 (6-C).

SPPS Synthesis of (2*R*,4′*R*,8a′*R*)-1-[*N*-(4-{[(5-Methylpyrazin-2-yl)carbonyl]amino}benzoyl)-β-alanyl]-6′-oxotetrahydro-2′*H*-spiro[pyrrolidine-2,7′-pyrrolo[2,1-*b*][1,3]thiazine]-4′-carboxamide, PAM6-SP20-BETA8-NH_2 (4). The peptidomimetic sequence was synthesized on Rink amide MBHA resin (66 mg, ~50 μmol), as described in typical procedures (Steps 1–4 of SPPS synthesis of **2**). Cleavage and purification of the crude product by RP-HPLC gave **4** (5.5 mg, 17.5%); analytical HPLC showed a peak related to the product at 8.87 min, purity > 95%. Mass value agrees with theoretical value: ESIMS *m*/*z* 566.23 $(M + H)^+$, 588.35 $(M + Na)^+$. ^{1}H NMR (Figure I in Supporting Information reports numbering system used for the attribution of main signals, 500 MHz, DMSO-d_6): δ 1.55–1.66 (m, 1H, 3-CH″), 1.84–2.00 (m, 3H, 9-CH″, 10-CH″, 6-CH″), 1.99–2.12 (m, 2H, 9-CH″, 10-CH″), 2.52–2.58 (m, 2H, 3-CH″, 13-CH″), 2.65 (s, 3H, 25-CH_3), 2.66–2.85 (m, 4H, 4-CH_2, 6-CH″, 13-CH″), 3.35–3.55 (m, 3H, 11-CH″, 14-CH_2), 3.66 (t, J = 8.1 Hz, 1H, 11-CH″), 4.63 (d, J = 4.7 Hz, 1H, 2-CH), 5.00 (dd, J = 9.0, 2.6 Hz, 1H, 5-CH), 7.32 (s, 1H, 28-NH′), 7.55 (s, 1H, 28-NH″), 7.84 (d, J = 8.5 Hz, 2H, 17-CH, 17′CH), 8.01 (d, J = 8.5 Hz, 2H, 18-CH, 18′-CH), 8.42 (t, J = 5.5 Hz, 1H, 27-NH), 8.72 (s, 1H, 24-CH), 9.18 (s, 1H, 22-CH), 10.85 (s, 1H, 26-NH); ^{13}C NMR (125.67 MHz, DMSO-d_6): δ 22.18 (25-C), 24.45 (10-C), 25.68 (3-C), 25.99 (4-C), 34.89 (13-C), 36.16 (14-C), 37.88 (6-C), 38.51 (9-C), 48.37 (11-C), 52.10 (2-C), 55.08 (5-C), 66.25 (7-C), 120.42 (18-C, 18′-C), 128.53 (17-C, 17′-C), 130.43 (16-C), 141.54 (19-C), 142.86 (21-C), 143.49 (24-C), 143.84 (22-C), 158.12 (23-C), 162.86 (20-C), 166.45 (15-C), 170.10 (12-C), 170.86 (1-C), 172.73 (8-C).

Synthesis of {(5*S*)-1-[(9*H*-Fluoren-9-yl-methyloxy)-carbonyl]-6-oxo-1,7-diazaspiro[4.5]dec-7-yl}-acetic Acid, Fmoc-BETA3-OH (33). (3*R*,7a*S*)-7a-But-3-en-1-yl-3-*tert*-butyltetrahydro-1*H*-pyrrolo[1,2-*c*][1,3]oxazol-1-one (25). Compound **25** was prepared according to the literature (yield 50%).[11c] TLC solvents: *n*-hexane/AcOEt 8/2, R_f 0.62. ^{1}H NMR (300 MHz, $CDCl_3$): δ 0.88 (s, 9H), 1.55–2.02 (m, 5H), 2.02–2.35 (m, 3H), 2.82–3.05 (m, 2H), 4.25 (s, 1H), 4.92–5.12 (m, 2H), 5.72–5.95 (m, 1H).

(*S*)-2-But-3-en-1-yl-proline (26). Compound **26** was prepared according to the literature (yield 60%).[11c] Mp 276–277 °C (lit.[11c] mp 281–282 °C dec). $[\alpha]^{20}_D$ = –70.2 (*c* 1.0, MeOH). ^{1}H NMR: (300 MHz, DMSO-d_6): δ 1.52–2.10 (m, 7H), 2.19–2.23 (m, 1H), 2.94–3.15 (m, 1H), 3.16–3.22 (m, 1H), 4.88–4.99 (m, 2H), 5.67–5.82 (m, 1H), 8.55 (bs, 1H). ESIMS *m*/*z* 192.2 $(M + Na)^+$.

(*S*)-2-But-3-en-1-yl-N-(*tert*-butoxycarbonyl)-proline (27). Compound **27** was prepared according to the literature (yield 93%).[11c] mp 86–88 °C (lit.[11c] mp 90–91 °C). $[\alpha]^{20}_D$ = +36.8 (*c* 2.0, MeOH). ^{1}H NMR (300 MHz, $CDCl_3$): δ 1.48, 1.53 (s, 9H), 1.70–1.92 (m, 2H), 1.92–2.20 (m, 4H), 2.20–2.40 (m, 1H), 2.75–2.85 (m, 1H), 3.25–3.45 (m, 1H), 3.45–3.62 (m, 1H), 4.94–5.14 (m, 2H), 5.71–5.94 (m, 1H), 10.95 (bs, 1H). ESIMS *m*/*z* 292.3 $(M + Na)^+$.

(*S*)-2-But-3-en-1-yl-N-(*tert*-butoxy-carbonyl)-prolylglycine Methyl Ester (28). (*S*)-2-But-3-en-1-yl-*N*-(*tert*-butoxycarbonyl)-proline **27** (8.0 g, 29.7 mmol), glycine methylester hydrochloride (3.7 g, 29.7 mmol), and hydroxybenzotriazole (4.0 g, 29.7 mmol) were solubilized in 100 mL of anhydrous $CHCl_3$. TEA (4.1 mL, 29.7 mmol) and then DCC (6.1 g, 29.7 mmol), dissolved in 100 mL of anhydrous $CHCl_3$, were added to the solution. The reaction mixture was left under stirring overnight at room temperature in an N_2 atmosphere. The dicyclohexylurea (DCU) formed was filtered, and the filtrate was then brought to dryness at reduced

pressure. The residue obtained was then shaken with Et_2O and filtered to eliminate any DCU; the liquid phase was washed with $NaHCO_3$ 1M, brine, 10% citric acid and then again with brine. The organic phase was dried over anhydrous Na_2SO_4, and the solvent was evaporated under reduced pressure, obtaining 13 g of a yellow oil that was purified using a silica gel chromatography column, eluting with *n*-hexane/AcOEt 2/1, R_f 0.65. Purification yielded **24** as a white solid (9.4 g, 93%). TLC solvents: *n*-hexane/AcOEt 2/1. $[\alpha]^{20}_D = -12.8$ (*c* 0.7, MeOH). ^{1}H NMR (300 MHz, $CDCl_3$): δ 1.54, 1.60 (2s, 9H), 1.75 (m, 3H), 2.10 (m, 4H), 2.75 (m, 1H), 3.35 (m, 1H), 3.58 (m, 1H), 3.75 (s, 3H), 4.05 (m, 2H), 5.00 (m, 2H), 5.82 (m, 1H), 6.50, 8.32 (2sa, 1H). ESIMS *m*/*z* 363.4 $(M + Na)^+$.

(5*S*)-7-(2-Methoxy-2-oxoethyl)-6-oxo-1,7-diazaspiro[4.5]decano-1-carboxylic Acid *tert*-Butyl Ester (30). (*S*)-2-But-3-en-1-yl-*N*-(*tert*-butoxycarbonyl)-prolylglycine methyl ester **28** (9.15 g, 27.0 mmol) was dissolved in 300 mL of MeOH/H_2O 2/1. OsO_4 (0.33 g, 1.3 mmol) was added to the solution and left stirring for 10 min, after bubbling of N_2, while adding $NaIO_4$ (17.1 g, 80.0 mmol) portionwise. A white precipitate formed from the dark-colored solution, and it was left stirring at room temperature for 24 h. H_2O was added to the reaction mixture until a solution was obtained and then it was extracted several times with AcOEt. The pooled organic phases were washed with H_2O, dried over anhydrous Na_2SO_4, and the solvent was evaporated under reduced pressure, obtaining 9.2 g of a mixture of the diastereoisomers of (5*R*)-8-hydroxy-7-(2-methoxy-2-oxoethyl)-6-oxo-1,7-diazaspiro[4.5]-decano-1-carboxylic acid *tert*-butyl ester **29** as a dark-colored oil. TLC solvent: AcOEt; R_f 0.39 and 0.52 (diastereoisomers). ^{1}H NMR (300 MHz, $CDCl_3$): δ 1.40, 1.48 (s, 9H), 1.60–1.65 (m, 1H), 1.65–2.00 (m, 4H), 2.08 (m, 1H), 2.10–2.80 (m, 2H), 3.25–3.40 (m, 1H), 3.50–, 3.70 (m, 2H), 3.75 (s, 3H), 4.05 (m, 2H), 8.20 (bs, 1H). This product was allowed to react without any further purification.

(5*R*)-8-Hydroxy-7-(2-methoxy-2-oxoethyl)-6-oxo-1,7-diazaspiro[4.5]decano-1-carboxylic acid *tert*-butyl ester **29** (9.0 g, 26.0 mmol) was dissolved in 180 mL of anhydrous THF. Trifluoroacetic acid (18 mL) was added to the solution, which was cooled in an ice bath before adding $NaBH_3CN$ (4.68 g, 74.0 mmol). The reaction mixture was left stirring for 20 h at room temperature under a nitrogen atmosphere and then alkalinized with K_2CO_3. The solution was separated from the residue by filtration, and the filtrate was then brought to dryness under reduced pressure. The amorphous mass obtained was dissolved in H_2O and extracted several times with CH_2Cl_2. The organic phase was dried over anhydrous Na_2SO_4, and the solvent was evaporated under reduced pressure. A total of 9 g of **30** was obtained as a dark-colored oil that was purified by silica column chromatography, eluting with *n*-hexane/AcOEt 1/3 to obtain **30** as a light-colored oil (4.5 g, 53%). TLC solvent: AcOEt, R_f 0.58. $[\alpha]^{20}_D = -58.6$ (*c* 1.3, MeOH). ^{1}H NMR (300 MHz, $CDCl_3$): δ 1.40, 1.60 (s, 9H), 1.60–2.15 (m, 6H), 2.15–3.80 (m, 2H), 3.30 (m, 1H), 3.30–3.80 (m, 4H), 3.75, 3.76 (2s, 3H), 4.70, 4.78 (2d, 1H). ESIMS *m*/*z* 349.2 $(M + Na)^+$.

[(5*S*)-1-(*tert*-Butoxycarbonyl)-6-oxo-1,7-diazaspiro[4.5]dec-7-yl]-acetic Acid (31). (5*S*)-7-(2-Methoxy-2-oxoethyl)-6-oxo-1,7-diazaspiro[4.5]decano-1-carboxylic acid *tert*-butyl ester **30** (4.0 g, 12.0 mmol) was dissolved in a solution of 60 mL of MeOH and 60 mL of H_2O, and then K_2CO_3 (3.32 g, 24.0 mmol) was added. The reaction mixture was kept at room temperature under stirring for 20 h, then brought to pH 5 with HCl 2 N, and evaporated under reduced pressure. The residue obtained was dissolved in H_2O, brought to pH 2–3, and extracted several times with CH_2Cl_2. The organic phase was dried over anhydrous Na_2SO_4, and the solvent was evaporated under reduced pressure, obtaining **31** as a white solid (3.2 g 86%). TLC solvents: $CHCl_3$/MeOH/AcOH 7.95/1.95/0.1, R_f 0.65. $[\alpha]^{20}_D = -58.4$ (*c* 0.5, MeOH). ^{1}H NMR (300 MHz, $CDCl_3$): δ 1.43 (s, 9H), 1.60–2.15 (m, 6H), 2.15–2.50 (m, 2H), 3.25 (m, 1H), 3.30–3.80 (m, 4H), 4.43, 4.98 (2d, 1H). ESIMS *m*/*z* 335.3 $(M + Na)^+$.

(5*R*)-7-(Carboxymethyl)-6-oxo-7-aza-1-azoniaspiro[4.5]decano Trifluoroacetate (32). [(5*S*)-1-(*tert*-Butoxycarbonyl)-6-oxo-1,7-diazaspiro-[4.5]dec-7-yl]-acetic Acid **31** (3.1 g, 10.0 mmol) was dissolved in a solution of 60 mL of CH_2Cl_2 and 60 mL of trifluoroacetic acid, and the reaction solution was left stirring for 1 h at room temperature. Next, it was brought to dryness under reduced pressure at 30 °C, and the residue was collected with H_2O and brought to dryness again under reduced pressure, drying thoroughly with an oil pump, to obtain product **28** as a light-colored oil (3.1 g, 95%). TLC solvents: $CHCl_3$/isoPrOH/MeOH/H_2O/AcOH 4.2/0.7/2.8/1.05/1.05, R_f 0.4. ^{1}H NMR (300 MHz, D_2O): δ 1.85–2.30 (m, 8H), 3.20–3.60 (m, 4H), 4.05 (d, 2H). ESIMS *m*/*z* 214.2 $(M + H)^+$.

{(5*S*)-1-[(9*H*-Fluoren-9-yl-methyloxy)-carbonyl]-6-oxo-1,7-diazaspiro[4.5]dec-7-yl}-acetic Acid (33). (5*R*)-7-(Carboxymethyl)-6-oxo-7-aza-1-azoniaspiro-[4.5]decano trifluoroacetate **32** (3.2 g, 10.0 mmol) was dissolved in 100 mL of H_2O. $NaHCO_3$ (1.7 g, 20.0 mmol) and then Fmoc-*N*-OSu (3.7 g, 11.0 mmol), dissolved in 150 mL of acetone, was added to the solution. The reaction mixture was left stirring at room temperature for 24 h, and after evaporating the acetone under reduced pressure, it was diluted with H_2O and washed with Et_2O. The aqueous phase was brought to pH 2–3 with HCl 2 N and extracted with $CHCl_3$; the organic phase was dried over anhydrous Na_2SO_4, and the solvent was evaporated under reduced pressure. The product obtained was crystallized with CH_2Cl_2 and Et_2O, thus obtaining **33** as a white solid (1.4 g, 32%). TLC solvents: $CHCl_3$/MeOH/AcOH 7.95/1.95/0.1, R_f 0.8.; mp 122–123 °C. $[\alpha]^{20}_D = -26.4$ (*c* 0.5, MeOH). HPLC: Symmetry C18 (5μ) column, 3.9 × 150 mm; mobile phase, KH_2PO_4 50 mM pH 3/CH_3CN 65/35; flow rate, 1.0 mL/min, RT, 5.2 min. ^{1}H NMR (300 MHz, $CDCl_3$): δ 1.20, 1.38, 1.62 (3m, 1H), 1.78–2.20 (m, 5H), 2.22–2.50 (m, 2H), 2.80, 3.45 (2m, 1H), 3.25 (m, 1H), 3.60 (dd, 1H), 3.65 (m, 1H), 3.80, 3.85 (2d, 1H), 4.15, 5.2 (2m, 1H), 4.2–4.35 (m, 1H), 4.40 (m, 1H), 4.60 (m, 1H), 7.20–7.45 (m, 8H), 7.58 (m, 2H), 7.75 (d, 2H). ESIMS *m*/*z* 457.4 $(M + Na)^+$. Anal. ($C_{25}H_{26}N_2O_5$) C, H, N. C: calcd, 69.10; found, 67.81; H: calcd, 6.03; found, 5.90; N: calcd, 6.44; found, 6.31.

SPPS Synthesis of *N*-{3-[(5*R*)-7-(2-Amino-2-oxoethyl)-6-oxo-1,7-diazaspiro[4.5]dec-1-yl]-3-oxopropyl}−4-[(1-naphthylacetyl)amino]benzamide, PAM8-SP20-BETA3-NH2 (5). The peptidomimetic sequence was synthesized on Rink amide MBHA resin (66 mg, ~50 μmol), as described in typical procedures (Steps 1–4 of SPPS synthesis of **2**), using **33**, prepared according to Scheme 6. Cleavage and purification of the crude product by RP-HPLC gave **5** (3.5 mg, 11.6%); analytical HPLC showed a peak related to the product at 10.02 min, purity > 94%. Mass value agrees with theoretical value: ESIMS *m*/*z* 570.17 $(M + H)^+$, 592.36 $(M + Na)^+$. ^{1}H NMR (Figure I in Supporting Information reports numbering system used for the attribution of main signals, 500 MHz, DMSO-d_6): δ 1.65–2.06 (m, 7H, 5-CH″, 6-CH_2, 9-CH_2, 13-CH_2), 2.25 (td, J = 12.7, 4.4 Hz, 1H, 5-CH″), 2.39–2.48 (m, 1H, 8-CH″), 2.54–2.66 (m, 1H, 8-CH″), 3.21–3.28 (m, 1H, 10-CH″), 3.34 (d, J = 16.6 Hz, 1H, 2-CH″), 3.36–3.54 (m, 4H, 12-CH_2, 10-CH″, 7-CH″), 3.63–3.70 (m, 1H, 7-CH″), 4.18 (s, 2H, 20-CH_2), 4.37 (d, J = 16.6 Hz, 1H, 2-CH″), 7.20 (s, 1H, 33-NH′), 7.29 (s, 1H, 33-NH″), 7.46–7.60 (m, 4H, 29-CH, 30-CH, 23-CH, 28-CH), 7.68 (d, J = 8.8 Hz, 2H, 17-CH, 17′-CH), 7.79 (d, J = 8.7 Hz, 2H, 16-CH, 16′-CH), 7.86 (dd, J = 7.6, 1.3 Hz, 1H, 24-CH), 7.95 (dd, J = 8.6, 1.3 Hz, 1H, 22-CH), 8.13 (d, J = 8.3 Hz, 1H, 27-CH), 8.27 (t, J = 5.7 Hz, 1H, 32-NH), 10.54 (s, 1H, 31NH); ^{13}C NMR (125.67 MHz, DMSO-d_6): δ 21.23 (6-C), 24.02 (9-C), 31.93 (5-C), 35.03 (8-C), 36.15 (12-C), 37.29 (13-C), 41.36 (20-C), 48.92 (7-C), 49.26 (10-C), 52.09 (2-C); 66.43 (4-C), 118.97 (17-C, 17′-C), 124.89 (27-C), 126.25 (29-C), 126.41 (23-C), 126.85 (28-C), 128.02 (24-C), 128.62 (30-C), 128.70 (16-C, 16′-C), 129.15 (22-C), 129.58 (15-C), 132.71 (25-C), 132.92 (26-C), 134.09 (21-C), 142.47 (18-C), 166.31 (14-C), 169.76 (11-C), 170.11 (19-C), 170.81 (3-C), 171.78 (1-C).

SPPS Synthesis of (2*R*,4′*R*,8a′*R*)-1-[(3-{[(4-Chlorophenoxy)-acetyl]amino}−1*H*-1,2,4-triazol-5-yl)carbonyl]-6′-oxotetrahydro-2′*H*-spiro[pyrrolidine-2,7′-pyrrolo[2,1-*b*][1,3]thiazine]-4′-carboxamide, PAM8-SP33-BETA8-NH$_2$ (6). The peptidomimetic sequence was synthesized on Rink amide MBHA resin (66 mg, ~50 μmol), as described in typical procedures (Steps 1–4 of SPPS

synthesis of **2**). Cleavage and purification of the crude product by RP-HPLC gave **6** (1.3 mg, 4.53%); analytical HPLC showed a peak related to the product at 10.08 min, purity > 93%. Mass value agrees with theoretical value: ESIMS *m/z* 534.17 $(M + H)^+$, 556.27 $(M + Na)^+$. ^{1}H NMR (Figure I in Supporting Information reports numbering system used for the attribution of main signals, 500 MHz, DMSO-d_6): δ 1.90–2.08 (m, 5H, 9-CH_2, 10-CH_2, 6-CH″), 2.53–2.57 (m, 2H, 3-CH_2), 2.67–2.83 (m, 3H, 6-CH", 4-CH_2), 3.50–3.58 (m, 1H, 11-CH″), 3.67–3.74 (m, 1H, 11-CH"), 4.62 (dd, $J = 5.8$, 1.70 Hz, 1H, 2-CH), 4.76 (d, $J = 15.6$ Hz, 1H, 16-CH″), 4.82 (d, $J = 15.6$ Hz, 1H, 16-CH"), 5.00 (dd, $J = 9.4$, 2.8 Hz, 1H, 5-CH), 6.94 (d, $J = 9.2$ Hz, 2H, 18-CH, 18′-CH), 7.09 (bs, 1H, 22-NH), 7.13 (bs, 1H, 19-NH′), 7.23 (bs, 1H, 19-NH"), 7.32 (d, $J = 9.2$ Hz, 2H, 19-CH, 19′-CH), 7.51 (bs, 1H, 21-NH); ^{13}C NMR (125.67 MHz, DMSO-d_6): δ 24.88 (10-C), 25.94 (3-C), 26.18 (4-C), 37.88 (6-C), 38.28 (9-C), 47.29 (11-C), 52.31 (2-C), 55.22 (5-C), 67.01 (7-C), 67.27 (16-C), 117.43 (18-C, 18′-C), 125.66 (20-C), 130.10 (19-C, 19′-C), 157.78 (17-C), 166.90 (15-C), 168.92 (12-C), 171.04 (1-C), 172.69 (8-C).

Biology. Yeast 2-Hybrid Assay. The vectors (pGBKT7 and pGADT7) used for the expression of MyD88 fused with the AD and BD domains were supplied by Clontech, as was the yeast strain AH109 (MATa, trp1-901, leu2-3 112, ura3-52, his3-200, gal4Δ, gal80Δ) and the minimal media SGd/-Leu/-Trp e SGd/-Ade/-His/-Leu/-Trp. The 384-well plates used for the assay were supplied by BD Biosciences (Oxygen BioSensor Plates), and the instrument for fluorescence measurements was the Fusion fluorescence detector (PerkinElmer). The AH109 yeast strain, cotransformed with the two gene fusions (AD-MyD88 and BD-MyD88), was preinoculated in 2 mL of SGd/-Leu/-Trp and incubated overnight at 30 °C under stirring at 200 rpm; the preinoculum was then diluted (1/20) in 100 mL of SGd/-Ade/-His/-Leu/-Trp for each well of the 384-well plates in the presence of the molecule to be assayed (final concentration: 100 μM). The plate was incubated in the Fusion instrument at 30 °C and the fluorescence emitted by each individual well was measured using an excitation wavelength of 485 nm, reading the emission at 630 nm from the bottom of the plate every 90 min for a total of 25 readings. Fluorescence intensity is an arbitrary unit, therefore, normalization is necessary: the fluorescence intensity of a well at a given time *t* must be divided by the initial fluorescence intensity of the same well.

Biology. NF-κB Inhibition Assay. HeLa (ECACC nr 93021013) cells were cultured in EMEM medium supplemented with 2 mM glutamine, 1% nonessential amino acids, 7.5% FBS (Fetal Bovine Serum) and 10 mL/L of a solution of penicillin/streptomycin (10000 units/mL penicillin and 10 mg/mL streptomycin). All reagents described were provided by Sigma-Aldrich. Cells were seeded in six-well plates at a density of 3×10^5 cells/well in complete medium and incubated overnight at 37 °C, 5% CO_2. After 18 h, cells were washed twice with PBS and then resuspended with 1 mL/well of EMEM without serum.

The compounds, dissolved in DMSO, were subsequently added to the cells at a final concentration of 100 μM, with the cells incubated for 6 h at 37 °C, 5% CO_2. The cells were stimulated with 5 ng/mL of recombinant human IL-1α (Sigma-Aldrich) for 30 min at 37 °C, 5% CO_2. After stimulation with IL-1α, the cells were washed twice with PBS, collected by cell scraping, and centrifuged at 800 rpm at 4 °C for 10 min. Activation/inhibition of NF-κB was evaluated by using the TransAM NF-κB p65 Kit (Active Motif) that allows detection of activated NF-κB through a colorimetric reaction.[27] Pellets were resuspended in lysis buffer (provided by kit), incubated for 10 min at 4 °C, and centrifuged at maximum speed at 4 °C. About 10 μg of total proteins, measured by Bradford Assay (BioRad), were utilized to perform these experiments. Percentage of inhibition is calculated by processing the values obtained in the spectrophotometric readings as follows: 100 − (IL* − C*/IL − C) = % inhibition of NF-κB, where IL* = A450 of cells stimulated and treated with the molecules under investigation; C* = A450 of cells not stimulated and treated with the molecules; IL = A450 of cells stimulated with IL-1α and not treated with the molecules; and C = A450 of cells neither stimulated nor treated. The compounds considered positive in the NF-κB inhibition assay were those showing a percentage inhibition ≥15%. The toxicity of positive compounds was evaluated by MTT assay.[28]

Acknowledgment. The authors wish to thank Mr. Augusto Liberati and Dr. Silvia Vincenti for their valuable contribution and Ms. Marlene Deutsch for editing the manuscript.

Supporting Information Available: Elemental analysis data, complete peptidomimetic sequences analytical data, ^{1}H NMR and ^{13}C NMR spectra, HPLC and ESIMS tracings of target compounds, and activity of reference compound BAY 11-7085. This information is available free of charge via the Internet at http://pubs.acs.org.

References

(1) Ghosh, S.; May, M. J.; Kopp, E. B. NF-kappa B and Rel proteins: Evolutionarily conserved mediators of immune responses. *Annu. Rev. Immunol.* **1998**, *16*, 225–260.
(2) Barnes, P. J.; Karin, M. Nuclear factor-kappaB: A pivotal transcription factor in chronic inflammatory diseases. *New Engl. J. Med.* **1997**, *336*, 1066–1071.
(3) O'Neill, L. A. J.; Dinarello, C. A. The IL-1 receptor/toll-like receptor superfamily: Crucial receptors for inflammation and host defense. *Immunol. Today* **2000**, *21*, 206–209.
(4) Loiarro, M.; Sette, C.; Gallo, G.; Ciacci, A.; Fantò, N.; Mastroianni, D.; Carminati, P.; Ruggiero, V. Peptide-mediated interference of TIR domain in MyD88 inhibits interleukin-1-dependent activation of NF-κB. *J. Biol. Chem.* **2005**, *280*, 15809–15814.
(5) Toshchakov, V. U.; Basu, S.; Fenton, M. J.; Vogel, S. N. Differential involvement of BB loops of Toll-IL-1 resistance (TIR) domain-containing adapter proteins in TLR4- versus TLR2-mediated signal transduction. *J. Immunol.* **2005**, *175*, 494–500.
(6) Li, C.; Zienkiewicz, J.; Hawiger, J. Interactive sites in the MyD88 Toll/Interleukin (IL) 1 receptor domain responsible for coupling to the IL1β signaling pathway. *J. Biol. Chem.* **2005**, *280*, 26152–26159.
(7) Fry, D. Protein−protein interactions as targets for small molecule drug discovery. *Biopolymers* **2006**, *84*, 535–552.
(8) Genin, M. J.; Ojala, W. H.; Gleason, W. B.; Johnson, R. L. Synthesis and crystal structure of a peptidomimetic containing the (*R*)-4.4-spiro lactam type-II β-turn mimic. *J. Org. Chem.* **1993**, *58*, 2334–2337.
(9) Long, R. D.; Moeller, K. D. Conformationally constrained peptide mimetics: The use of a small lactam ring as an HIV-1 antigen constraint. *J. Am. Chem. Soc.* **1997**, *119*, 12394–12395.
(10) Peña, M. R.; Stille, J. K. A total synthesis of anthramicin: Application of palladium-catalyzed coupling reactions for the attachment of the acrylic side chain. *J. Am. Chem. Soc.* **1989**, *111*, 5417–5424.
(11) (a) Seebach, D.; Boes, M.; Naef, R.; Schweizer, B. Alkylation of amino acids without loss of the optical activity: Preparation of α-substituted proline derivates. A case of self-reproduction of chirality. *J. Am. Chem. Soc.* **1983**, *105*, 5390–5398. (b) Genin, M. J.; Baures, P. W.; Johnson, R. L. An improved method of oxazolidinone hydrolysis in the asymmetric synthesis of α-alkylprolines. *Tetrahedron Lett.* **1994**, *23* (35), 4967–4968. (c) Khalil, E. M.; Ojala, W. H.; Pradhan, A.; Nair, V. D.; Gleason, W. B.; Mishra, R. K.; Johnson, R. L. Design, synthesis, and dopamine receptor modulating activity of spiro bicyclic peptidomimetics of L-prolyl-L-leucyl-glycinamide. *J. Med. Chem.* **1999**, *42*, 628–637.
(12) Lipinski, C. A.; Lombardo, F.; Dominy, B. W.; Feeney, P. J. Experimental and computational approaches to estimate solubility and permeability in drug discovery and development settings. *Adv. Drug Delivery Rev.* **1997**, *23*, 3–25.
(13) Olsson, I.-M.; Gottfries, J.; Wold, S. D-Optimal onion designs in statistical molecular design. *Chemom. Intell. Lab. Syst.* **2004**, *73*, 37–46.
(14) Ferguson, A. M.; Heritage, T.; Jonathon, P.; Pack, S. E.; Phillips, L.; Rogan, J.; Snaith, P. J. EVA: A new theoretically based molecular descriptor for use in QSAR/QSPR analysis. *J Comput.-Aided Mol. Des.* **1997**, *11*, 143–152.
(15) Bartfai, T.; Behrens, M. M.; Gaidarova, S.; Pemberton, J.; Shivanyuk, A.; Rebek, J., Jr. A low molecular weight mimic of the Toll/IL-1 receptor/resistance domain inhibits IL-1 receptor-mediated responses. *Proc. Natl. Acad. Sci. U.S.A.* **2003**, *100*, 7971–7976.
(16) (a) Fields, S.; Song, O. A novel genetic system to detect protein−protein interactions. *Nature* **1989**, *340*, 245–246. (b) Chien, C. T.; Bartel, P. L.; Sternglanz, R.; Fields, S. The two-hybrid system: a method to identify and clone genes for proteins that interact with a protein of interest. *Proc. Natl. Acad. Sci. U.S.A.* **1991**, *88*, 9578–9582.
(17) Wodnicka, M.; Guarino, R. D; Hemperly, J. J; Timmins, M. R; Stitt, D.; Pitner, J. B. Novel fluorescent technology platform for high

throughput cytotoxicity and proliferation assays. *J. Biomol. Screen.* **2000**, *5*, 141–152.
(18) Pierce, J. W.; Schoenleber, R.; Jesmok, G.; Best, J.; Moore, S. A.; Collins, T. E.; Gerritsen, M. E. Novel inhibitors of cytokine induced IκBα phosphorylation and endothelial cell adhesion molecule expression show anti-inflammatory effects in vivo. *J. Biol. Chem.* **1997**, *272*, 21096–21103.
(19) Loiarro, M.; Capolunghi, F.; Fantò, N.; Gallo, G.; Campo, S.; Arseni, B.; Carsetti, R.; Carminati, P.; De Santis, R.; Ruggiero, V.; Sette, C. Inhibition of MyD88 dimerization and recruitment of IRAK1 and IRAK4 by a novel peptidomimetic compound. *J. Leukocyte Biol.* **2007**, *82*, 801–810.
(20) (a) Hoffman, E. S.; Smith, R. E.; Renaud, R. C., Jr. TLR-targeted therapeutics. *Nat. Rev.* **2005**, *4*, 879–880. (b) Wickelgren, I. Targeting the tolls. *Science* **2006**, *312*, 184–187. (c) Gearing, A. J. H. Targeting toll-like receptors for drug development: A summary of commercial approaches. *Immunol. Cell Biol.* **2007**, *85*, 490–494.
(21) Krieg, A. M. Therapeutic potential of Toll-like receptor 9 activation. *Nat. Rev. Drug Discovery* **2006**, *5*, 471–484.
(22) Ulevitch, R. J. Therapeutics targeting the innate immune system. *Nat. Rev. Immunol.* **2004**, *4*, 512–520.
(23) *TSAR3D*, v. 3.3; Accelrys Inc.: 9685 Scranton Road, San Diego, CA 92121–3752.
(24) *SIMCA-P*, v. 10.0; Umetrics AB: Box 7960, SE-90719 Umeå, Sweden.
(25) *MODDE*, v. 7.0; Umetrics AB: Box 7960, SE-90719 Umeå, Sweden.
(26) (a) Atherton, E.; Sheppard, R. C. The Fluorenylmethoxycarbonyl Amino Protective Group. In *The Peptides*; Udenfriend, S., Meienhofer, J., Eds.; Academic Press: New York, 1987; *Vol. 9*, pp 1–39. (b) Hanessian, S.; Lavalle, P. The preparation and synthetic utility of *tert*-butyldiphenylsilyl ethers. *Can. J. Chem.* **1975**, *53*, 2975–2977.
(27) Renard, P.; Ernest, I.; Houbion, A.; Art, M.; Le Calvez, H.; Raes, M.; Remacle, J. Development of a sensitive multi-well colorimetric assay for active NFkappaB. *Nucleic Acids Res.* **2001**, *29*, e21.
(28) Mosmann, T. J. Rapid colorimetric assay for cellular growth and survival: Application to proliferation and cytotoxicity assays. *J. Immunol. Methods* **1983**, *65*, 55–63.

JM070723U